





Mitophagy receptor FUNDC1 is regulated by PGC-1 α /NRF1 to fine tune mitochondrial homeostasis

Lei Liu^{1,2,*} , Yanjun Li³, Jianing Wang³, Di Zhang^{1,2,3}, Hao Wu¹, Wenhui Li^{1,2}, Huifang Wei⁴, Na Ta^{1,2}, Yuyuan Fan^{1,2}, Yujiao Liu^{1,2}, Xiaohui Wang¹, Jun Wang¹, Xin Pan⁵ , Xudong Liao³, Yushan Zhu³  & Quan Chen^{3,**} 

Abstract

Mitophagy is an essential cellular autophagic process that selectively removes superfluous and damaged mitochondria, and it is coordinated with mitochondrial biogenesis to fine tune the quantity and quality of mitochondria. Coordination between these two opposing processes to maintain the functional mitochondrial network is of paramount importance for normal cellular and organismal metabolism. However, the underlying mechanism is not completely understood. Here we report that PGC-1 α and nuclear respiratory factor 1 (NRF1), master regulators of mitochondrial biogenesis and metabolic adaptation, also transcriptionally upregulate the gene encoding FUNDC1, a previously characterized mitophagy receptor, in response to cold stress in brown fat tissue. NRF1 binds to the classic consensus site in the promoter of *Fundc1* to upregulate its expression and to enhance mitophagy through its interaction with LC3. Specific knockout of *Fundc1* in BAT results in reduced mitochondrial turnover and accumulation of functionally compromised mitochondria, leading to impaired adaptive thermogenesis. Our results demonstrate that FUNDC1-dependent mitophagy is directly coupled with mitochondrial biogenesis through the PGC-1 α /NRF1 pathway, which dictates mitochondrial quantity, quality, and turnover and contributes to adaptive thermogenesis.

Keywords adaptive thermogenesis; brown adipose tissue; mitochondrial biogenesis; mitophagy

Subject Categories Membranes & Trafficking; Metabolism

DOI 10.15252/embr.202050629 | Received 13 April 2020 | Revised 27 November 2020 | Accepted 15 December 2020 | Published online 8 February 2021

EMBO Reports (2021) 22: e50629

Introduction

Mitochondria are highly dynamic and undergo constant turnover through two opposing processes: mitophagy, which selectively removes superfluous and damaged mitochondria by the autolysosomal pathway, and mitochondrial biogenesis, which generates fresh, functional ones (Gottlieb & Gustafsson, 2011; Palikaras & Tavernarakis, 2014; Dorn *et al.*, 2015; Pickles *et al.*, 2018). Mitochondrial biogenesis preserves mitochondrial function and cellular homeostasis under diverse (patho-)physiological conditions such as physical exercise, nutrient deprivation, temperature fluctuations (Rasbach & Schnellmann, 2007; Miwa *et al.*, 2008; Gottlieb & Carreira, 2010), and during cell differentiation (Chen *et al.*, 2012). On the other hand, mitophagy, by removing the “old” or damaged mitochondria, reduces the source of oxidative stress (Schofield & Schafer, 2020), limits the risk of cell senescence and apoptosis (Hickson-Bick *et al.*, 2008), and allows the cell to undergo metabolic reprogramming during developmental and environmental stress. However, excessive mitophagy in the absence of mitochondrial biogenesis causes stress to the remaining mitochondria and leads to mitophagic cell death (Dagda *et al.*, 2008; Kubli & Gustafsson, 2012; Gottlieb & Thomas, 2017; Manfredi *et al.*, 2019; Pirooznia *et al.*, 2020). Proper coordination of mitophagy and mitochondrial biogenesis is essential for the quantity and quality control of mitochondria and allows cells

1 State Key Laboratory of Membrane Biology, Institute of Zoology, Chinese Academy of Sciences, Beijing, China

2 University of Chinese Academy of Sciences, Beijing, China

3 College of Life Sciences, Nankai University, Tianjin, China

4 Department of Pathophysiology, School of Basic Medical Sciences, Zhengzhou University, Zhengzhou, Henan, China

5 Institute of Basic Medical Sciences, National Center of Biomedical Analysis, Beijing, China

*Corresponding author. Tel: +86 10 64807321; E-mail: liulei@ioz.ac.cn

**Corresponding author. Tel: +86 22 23506218; E-mails: chenq@nankai.edu.cn; chenq@ioz.ac.cn

to change their mitochondrial mass in response to the ever-changing cellular metabolic state and to intracellular or environmental cues (Palikaras *et al*, 2015a; Altshuler-Keylin & Kajimura, 2017). An imbalance between mitochondrial degradation and biogenesis leads to functional impairment of biological systems and cell death (Ploumi *et al*, 2017). The significance of coordination between these processes is further underlined by evidence showing that altered mitochondrial mass is a common feature of numerous pathologic conditions (Vafai & Mootha, 2012; Dorn *et al*, 2015). During aging and in many diseases, gradual changes in mitochondrial mass and progressive mitochondrial dysfunction are observed (Preston *et al*, 2008; Artal-Sanz & Tavernarakis, 2009; Kaeberlein, 2010; Palikaras *et al*, 2015a). Thus, the crosstalk between mitophagy and mitochondrial biogenesis is vital to maintain normal cellular and organismal physiology. Both mitophagy and mitochondrial biogenesis are emerging as potential targets for therapeutic interventions against diseases associated with aging (Valero, 2014; Palikaras *et al*, 2017).

Mitochondrial biogenesis is spatiotemporally regulated by activating different transcription factors. Among these are nuclear respiratory factors (NRF1 and NRF2) (Scarpulla, 1997, 2008), estrogen-related receptors (ERR- α , ERR- β , ERR- γ) (Fan & Evans, 2015), and myocyte enhancer factor 2 (MEF2) (Scarpulla, 2002). Their transcription activity is orchestrated by the peroxisome proliferator-activated receptor gamma co-activator 1-alpha (PGC-1 α) in response to diverse stimuli, such as hormones, growth factors, fasting/feeding transition, physical exercise, and temperature fluctuations (Anderson *et al*, 2008; Fernandez-Marcos & Auwerx, 2011; Miller *et al*, 2019). PGC-1 α acts as a sensor for different signaling pathways, which regulate its expression, phosphorylation, stability, and transcriptional activity (Kelly & Scarpulla, 2004; Dominy & Puigserver, 2013). Once activated, PGC-1 α is recruited to the chromatin where it physically interacts with or indirectly activates these transcriptional regulators, which are involved in diverse cellular functions including metabolic adaptation and mitochondrial biogenesis in a context-dependent manner (Puigserver, 2005; Scarpulla *et al*, 2012). For example, in brown adipose tissue (BAT), chronic cold exposure stimulates the β -adrenergic signaling pathway to activate PGC-1 α through post-translational modifications and increased expression of the PGC-1 α gene (Puigserver *et al*, 1998; Lowell & Spiegelman, 2000; Cannon & Nedergaard, 2004). Subsequently, the activated PGC-1 α enhances the transcription activities of NRF1 along with PPAR γ to drive mitochondrial biogenesis and adaptive metabolic gene programs leading to metabolic reprogramming and increased non-shivering energy expenditure. Notably, mice deficient in PGC-1 α are extremely cold-sensitive (Lin *et al*, 2004; Leone *et al*, 2005), and only half of PGC-1 α KO pups survive the early postnatal period and grow into adults (Lin *et al*, 2004). Deficiency of NRF1 caused embryonic lethality in mice (Huo & Scarpulla, 2001). These results highlight the important role of PGC-1 α and NRF1-mediated mitochondrial biogenesis in development and metabolic adaptations.

Significant advances have been made in understanding the regulation of mitophagy, mostly based on cultured cell systems (Ashrafi & Schwarz, 2013; Liu *et al*, 2014). Two major pathways have been described to mediate the recruitment of the autophagic machinery for subsequent degradation of mitochondria, one depending on PINK1/Parkin and the other relying on a set of receptor proteins such as FUNDC1, NIX, BCL2L13, FKBP8, and PHB2 (Novak *et al*, 2010; Liu *et al*, 2012; Okamoto, 2014; Murakawa *et al*, 2015;

Bhujabal *et al*, 2017; Wei *et al*, 2017; Lampert *et al*, 2019). Upon loss of mitochondrial membrane potential, or treatment with mitochondrial toxins or hypoxia, these pathways become activated to recruit other autophagy receptors and autophagy-related proteins (ATGs) including ULK1 to mitochondria for formation of mitophagosomes (Corti & Brice, 2013; Zhang & Lin, 2016; Laker *et al*, 2017). Loss of Parkin, NIX, FUNDC1, or ULK1 leads to the accumulation of functionally compromised and swollen mitochondria, indicative of defective mitophagy (Kundu *et al*, 2008; Sandoval *et al*, 2008; McWilliams & Muqit, 2017; Li *et al*, 2019). Surprisingly, however, there are other reports showing that dysfunctional mitochondria caused by the specific knockout of mitochondrial transcription factor A (Tfam) do not recruit Parkin *in vivo*, and neither the clearance of defective mitochondria nor the neurodegeneration phenotype is affected by the absence of Parkin (Sterky *et al*, 2011). Also, exercise-induced mitophagy in skeletal muscle occurs in the absence of stabilization of PINK1 on mitochondria (Drake *et al*, 2019). These results suggest that that Parkin and PINK1 do more than just activate mitophagy (Scarffe *et al*, 2014). Thus, the molecular regulation of mitophagy and its contribution to mitochondrial and cellular (patho-)physiology and aging or aging-related diseases requires further clarification.

Although the molecular regulation of both mitochondrial biogenesis and mitophagy is well characterized, it is less clear how these two opposing processes are coordinated to produce a functional mitochondrial network under (patho-)physiological settings. It is interesting to note that both mitochondrial biogenesis and mitophagy are induced in response to (patho-)physiological stimuli that are known to induce mito(auto-)phagy, such as nutrient deprivation, physical exercise (Memme *et al*, 2019), ischemia preconditioning (Gottlieb & Pourpirali, 2016), and other stresses (Rasbach & Schnellmann, 2007; Diaz & Moraes, 2008; Gottlieb & Carreira, 2010). It appears that mito(auto-)phagy and mitochondrial biogenesis share common signaling pathways (Jager *et al*, 2007; Canto & Auwerx, 2009; Birkenfeld *et al*, 2011). It was also suggested that mitophagy also impacts on mitochondrial biogenesis so to balance mitochondrial turnover. Knockout of NIX or BNIP3 leads to the increased mitochondrial mass (Dorn, 2010), while overexpression of Bnip3 reduces the levels of both nuclear- and mitochondrial-encoded proteins owing to the stimulation of mitochondrial turnover (Rikka *et al*, 2011). Parkin was found to regulate mitochondrial biogenesis through the regulation of PARIS (ZFN746), a zinc finger protein and a substrate of Parkin (Shin *et al*, 2011). In an effort to understand the mechanism of cold-induced mitophagy in brown fat tissue, we demonstrated that PGC-1 α /NRF1, two master regulators of mitochondrial biogenesis, also transcriptionally regulate FUNDC1. We showed that FUNDC1-dependent mitophagy is coupled with mitochondrial biogenesis, and defective mitophagy leads to abnormal mitochondrial turnover. We suggest that this regulation of FUNDC1 by PGC-1 α /NRF1 controls mitochondrial number, quality, and turnover, thereby contributing to thermogenesis in response to cold stress.

Results

Expression of FUNDC1 is induced by cold exposure in BAT

Brown adipose tissue (BAT) has a high abundance of mitochondria, and mitochondrial biogenesis is strongly induced during cold acclimation (Puigserver *et al*, 1998). Indeed, when mice were kept at 4°C for 3 days, compared to control mice which were housed under thermally neutral conditions (30°C), we observed that the levels of some mitochondrial proteins, such as cytochrome *c* (CYCS) and TIM23, were increased 1.7-fold (Fig 1A and B). Many of the corresponding mRNAs were also upregulated (Fig 1C). The mitochondrial uncoupling protein 1 (UCP1) was induced up to 3-fold (Fig 1A and B), while the induction of *Ucp1* mRNA was much higher than that of the protein (Fig 1C). This reflects the fact that *Ucp1* is transcriptionally regulated by both PGC-1 α and PPAR α (Barbera *et al*, 2001), and the half-life of *Ucp1* mRNA is dramatically reduced upon cold exposure (Jacobsson *et al*, 1987; del Mar Gonzalez-Barroso *et al*, 2000; Nedergaard *et al*, 2001). In agreement with a previous report in rats (Watanabe *et al*, 2008), VDAC1 is unaffected upon cold exposure in BAT in mice. We also found that the protein level, but not the mRNA level, of HSP60 is increased upon cold exposure, which indicates that some mitochondrial protein levels are subjected to post-transcriptional regulation in BAT. We also detected a two-fold increase in the mtDNA copy number (Fig 1D), further supporting the notion that mitochondrial biogenesis is induced upon cold exposure. The fold increases of mRNA, protein, and mtDNA levels are different, which suggests that distinct regulatory mechanisms are involved in gene expression and protein stability. Surprisingly, we also found a robust induction of FUNDC1, a previously characterized mitophagy receptor, at both the protein (2.6-fold) and mRNA (2.3-fold) levels in BAT after 3 days of cold exposure (Fig 1A–C). The relative increase of mitochondrial proteins was analyzed by normalizing proteins levels to the mtDNA levels, which showed that more FUNDC1 was induced compared to the other mitochondrial proteins, such as HSP60, TIM23, and VDAC1 (Fig 1E). The levels of NIX, another reported mitophagy receptor, were not affected at either the mRNA or protein levels (Fig 1A–C). The protein and mRNA levels of Parkin were significantly reduced upon cold exposure (Fig 1A–C), consistent with a previous report that Parkin expression is repressed by thermogenic stimuli (Cairo *et al*, 2019). We also found that the protein level of PINK1 was increased, while the mRNA level of PINK1 was reduced upon cold exposure (Fig 1A–C), which indicates the protein level of PINK1 is regulated by post-transcriptional mechanism (Jin *et al*, 2010; Greene *et al*, 2012; Cairo *et al*, 2019). Immunohistochemical analysis further confirmed the increased expression of FUNDC1 in BAT after cold exposure (Fig 1F and G).

PGC-1 α regulates FUNDC1 expression

It is well established that PGC-1 α and NRF1 are responsible for mitochondrial biogenesis in BAT in response to cold acclimation (Wu *et al*, 1999). We were thus prompted to examine whether they are responsible for the induction of FUNDC1. Some of the commercial antibodies against PGC-1 α are not suitable for Western blotting. After several tests, we found that the mouse monoclonal antibody 4C1.3 gives a consistent result in detecting a 113-kD PGC-1 α band in

Western blots (Aquilano *et al*, 2010; Ruas *et al*, 2012; Park *et al*, 2015). The levels of NRF1 and PGC-1 α proteins were increased by 1.6- to 3.8-fold in BAT after cold exposure (Fig 2A and B). The mRNA level of PGC-1 α was also significantly increased upon cold exposure; however, the mRNA level of NRF1 was unchanged, which suggests that the stability of NRF1 protein is increased by cold exposure or the increase of NRF1 mRNA occurs at an earlier time point (Fig 2C). It was reported that PGC-1 α expression is highly induced during brown adipocyte differentiation (Uldry *et al*, 2006). We thus wanted to know whether the expression of FUNDC1 is also induced during this process. We isolated brown fat preadipocytes from mice and immortalized these cells by infection with SV40 large T antigen. We found that, like UCP1 and CYCS, which are PGC-1 α -regulated proteins, the FUNDC1 protein level was elevated when the immortalized preadipocytes were treated with an adipogenic cocktail to induce their differentiation into brown adipocytes, while the protein level of VDAC1 was unchanged during the differentiation process (Fig EV1A–C). We then infected the immortalized brown preadipocytes cells with adenoviruses encoding PGC-1 α or GFP and found that the FUNDC1 protein level was markedly enhanced along with other PGC-1 α /NRF1-regulated gene products such as CYCS (Fig EV1D–F). The levels of other mitochondrial proteins such as TIM23 and VDAC1 were not affected by PGC-1 α re-introduction, which indicates that the induction of FUNDC1 is not due to the overall increase of mitochondrial content induced by PGC-1 α (Fig EV1D–F). Moreover, the FUNDC1 protein level was also elevated by 2- to 3-fold in HeLa and 293 cells when PGC-1 α was ectopically introduced (Fig EV1G and H), which suggests that PGC-1 α regulation of FUNDC1 is of general significance. Conversely, knockdown of PGC-1 α in the immortalized brown preadipocytes reduced the protein and mRNA levels of FUNDC1, and this effect could be rescued by reintroducing PGC-1 α into stable PGC-1 α knockdown brown preadipocytes (Fig 2D–F). We found that both in preadipocytes and in mature adipocytes, when PGC-1 α was knocked down, the level of the PGC-1 α -regulated mitochondrial protein CYCS also decreased like FUNDC1, although the expression of another mitochondrial protein, VDAC1, was unaffected (Fig 2D–H). The regulation of FUNDC1 expression by PGC-1 α is specific, as knockdown of its close homolog PGC-1 β , which also functions in mitochondrial biogenesis and regulation of energy expenditure, had no effect on FUNDC1 expression (Fig EV2A–C). Taking these results together, we conclude that the expression of FUNDC1 is specifically regulated by PGC-1 α .

NRF1 transcriptionally regulates FUNDC1 expression

Since PGC-1 α stimulates mitochondrial biogenesis through NRF1 in response to cold stress, we considered the possibility that FUNDC1 is transcriptionally regulated by NRF1. To pursue this, we identified two putative NRF1 binding sites in the promoter of the *Fundc1* gene using the online promoter analysis tool AliBaba2.1. These sites are located at -1315/-1305 and -186/-176 (Fig 3A). Deletion and mutation analysis identified that the -186/-176 NRF1 binding element is functional (Fig 3A and B). This site is identical to the sequence previously identified in the *VSNL1* promoter (Fu *et al*, 2009) and is required for *Fundc1* promoter activity (Fig 3A and B). To determine whether NRF1 directly binds to the *Fundc1* promoter, we performed electrophoretic mobility shift assay (EMSA) analysis with nuclear proteins extracted from HeLa cells. Firstly, we synthesized a positive

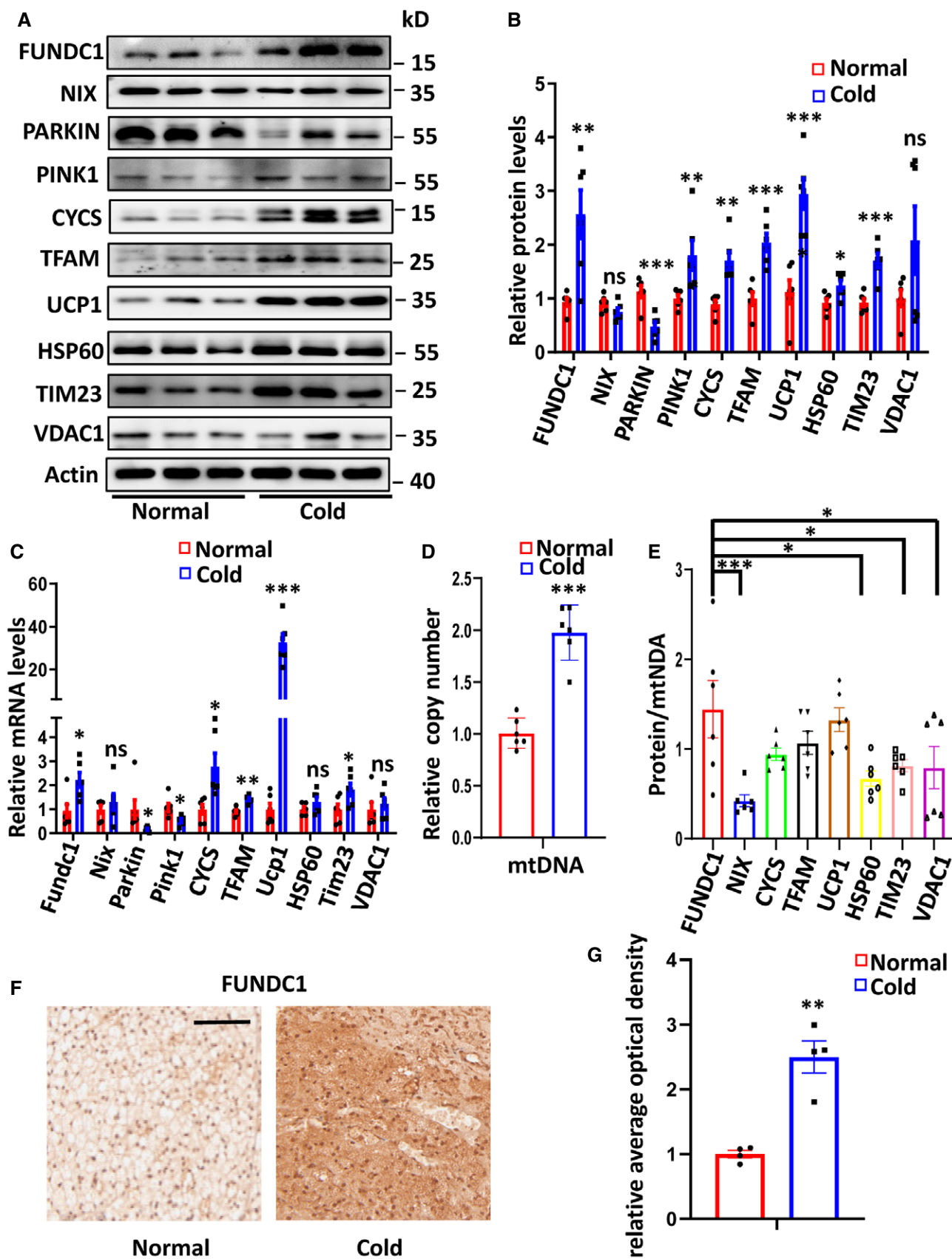


Figure 1.

Figure 1. Expression of FUNDC1 is induced by cold exposure in BAT.

- A–E BATs were isolated from cold-exposed mice (4°C, 72 h) or control mice (30°C, 72 h), then lysed, and subjected to Western blotting for analysis of the indicated proteins (A). Relative protein expression levels, normalized to actin, are shown in (B). mRNA expression levels of the indicated genes were assayed by real-time PCR and normalized to *Actb* (C). Mitochondrial DNA copy numbers were determined by real-time PCR and normalized to nuclear DNA standards (D). Relative increase of mitochondrial proteins was normalized to mtDNA copy numbers and plotted (E). Data information: $n = 6$ biological replicates, data are represented as the mean \pm SEM. Statistical analysis was performed using two-tailed Student's *t*-test. ns: no significant difference; * $P < 0.05$; ** $P < 0.01$; *** $P < 0.001$.
- F, G Representative images showing immunohistochemical detection of FUNDC1 in sections of BATs from mice kept at 30 or 4°C for 72 h. Scale bar, 50 μ m. The expression of FUNDC1 was quantified by analyzing and normalizing the average optical density of FUNDC1 staining. Data information: $n = 4$ biological replicates, data are represented as the mean \pm SEM. Statistical analysis was performed using two-tailed Student's *t*-test. ** $P < 0.01$.

control oligonucleotide probe according to the NRF1 binding site sequence in the *VSNL1* promoter (Fu *et al*, 2009) and compared it to an oligonucleotide probe containing the NRF1 binding sequence in the *Fundc1* promoter (*Fundc1* probe). The biotinylated *Fundc1* probe but not the mutant *Fundc1* probe was retarded in the same way as the positive control probe in the presence of HeLa nuclear proteins (Fig 3C). Furthermore, the retarded band was competitively blocked by a cold oligonucleotide but not by a mutant oligonucleotide (Fig 3D). A super-shifted band was observed when an NRF1 antibody was added, which indicates that NRF1 binds to the *Fundc1* promoter (Fig 3D). We further performed ChIP-PCR analysis with the NRF1 antibody on the *Fundc1* promoter to verify NRF1 binding to the *Fundc1* promoter in HeLa cells (Fig 3E). Additionally, in the immunoprecipitate of Flag-PGC-1 α -transfected cells, we were able to detect the region of the *Fundc1* promoter containing the NRF1 binding element, which indicates cobinding of PGC-1 α and NRF1 on the *Fundc1* promoter in HeLa cells (Fig 3F). Next, we asked whether NRF1 was responsible for the expression of FUNDC1 in cells. The protein level of FUNDC1 was reduced in NRF1 stable knockdown HeLa cells, and this reduction was rescued by reintroducing NRF1 (Fig 3G). We also confirmed that the expression of FUNDC1 was also regulated by NRF1 in mature adipocytes, while the level of the FUNDC1 protein decreased when NRF1 was knocked down (Fig EV2D and E). Also, the induction of FUNDC1 by PGC-1 α was partially suppressed by knockdown of NRF1 (Fig 3H). Finally, by ChIP-PCR, we showed that PGC-1 α binding on the *Fundc1* promoter was also compromised in NRF1 stable knockdown cells (Fig 3I). Together, these data demonstrated that the PGC-1 α /NRF1 axis is responsible for transcriptional regulation of the expression of FUNDC1.

Cold exposure induces mitophagy and the interaction between FUNDC1 and LC3

The robust induction of FUNDC1 in BAT after cold exposure prompted us to examine whether mitophagy is also induced in a FUNDC1-dependent manner. Early studies suggested that cold suppresses autophagy (Cairo *et al*, 2016). However, recent studies showed that some (if not all) ATG genes are induced upon cold exposure (Martinez-Lopez *et al*, 2016; Lu *et al*, 2018). Western blotting analysis showed that several autophagy marker proteins, including ATG5, ULK1, LC3B (Kabeya *et al*, 2000), and the lipidated form of LC3B (LC3BII) (He & Klionsky, 2009), were drastically elevated in BAT upon cold challenge (Fig 4A and B). The mRNA levels of the corresponding ATG genes were also moderately increased (Fig EV2F). We found that the protein levels of both AMPK α and phosphorylated AMPK α (at Thr172) are enhanced upon

cold exposure, which suggests that activation of AMPK α is involved in the induction of autophagic flux by cold (Fig 4A and B). Immunostaining further confirmed that expression of the autophagy marker LC3B was induced in BAT after cold exposure (Fig 4C). Next, we treated mice with chloroquine for 72h and found that the LC3B-II levels upon cold exposure were significantly higher than that treated with chloroquine at 30°C, indicating the induction of autophagic flux upon cold exposure (Fig EV2G and H). To ascertain that mitophagy occurs, we acquired electron microscope (EM) images to assess the ultrastructure of BAT mitochondria and mitophagosomes from mice subjected to 4°C (cold) versus 30°C (normal) for 3 days. We clearly observed that some mitochondria with typical cristae were engulfed by autophagosomes in the cold-exposed BAT (Fig 4D). Compared to controls, the number of mitophagosomes was significantly increased upon cold challenge (Fig 4D and E). These results indicate that mitophagy is significantly increased in cold-exposed BAT.

As both FUNDC1 and LC3B are induced in cold-challenged BAT, we next wanted to know whether the interaction between FUNDC1 and LC3B is enhanced upon cold exposure. By using co-immunoprecipitation, we found that about double the amount of LC3B protein was immunoprecipitated by FUNDC1 and 1.7-fold of FUNDC1 protein was immunoprecipitated by LC3B during cold exposure (Fig 4F and G). This suggests that the interaction between FUNDC1 and LC3B was increased in mouse BAT under cold conditions (Fig 4F and G).

FUNDC1 is required for cold-induced mitophagy in mouse BAT

To determine the contribution of FUNDC1 to mitophagy in BAT, we generated brown adipocyte-specific *Fundc1* knockout mice by crossing *Fundc1*^{fl/fl} mice with a *Ucp1*^{cre+} transgenic mouse (Kong *et al*, 2014). The genotypes of these mice were identified by PCR, and specific knockout of *Fundc1* in brown adipose tissue was verified by Western blotting (Fig EV3A). The BAT-specific *Fundc1* knockout mice were normal, and there was no significant difference in O₂ consumption and CO₂ production rates between control (Cre⁻) and BAT-specific *Fundc1* knockout mice when the animals were maintained at 30°C (Fig EV3B and C). EM analysis revealed that the appearance of mitophagosomes was suppressed in BAT of cold-exposed *Fundc1*^{fl/fl}/*Ucp1*^{cre+} mice (Fig 5A and B), which supports the idea that FUNDC1 plays a role in cold-induced mitophagy. We also found that the increase in autophagy proteins upon cold exposure was unaffected by FUNDC1 deficiency, indicating that FUNDC1 is mainly responsible for mitophagy in BAT (Fig EV4A and B). To firmly establish that mitophagy is indeed activated along with mitochondrial biogenesis *in vivo*, we generated adipocyte-specific

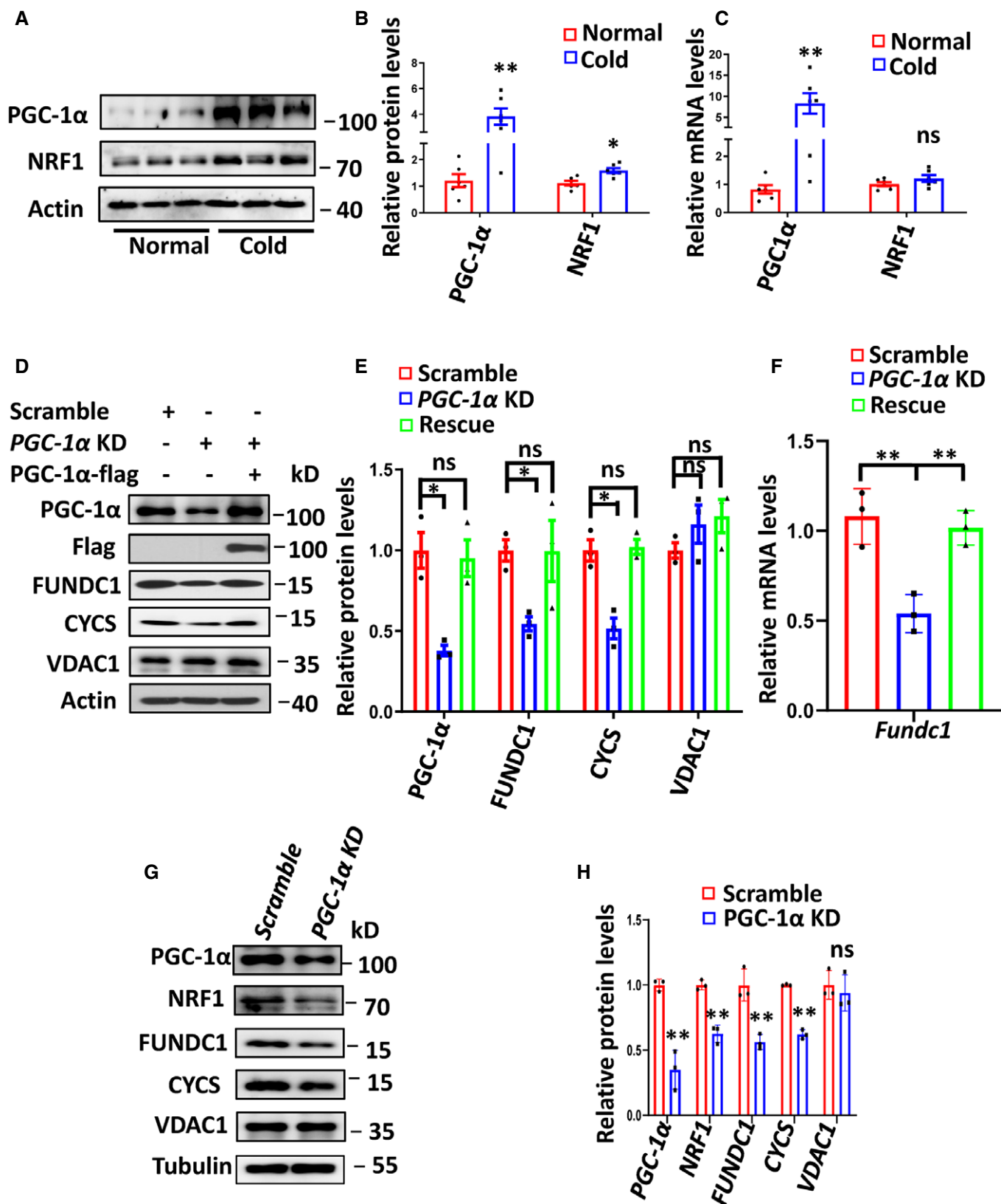


Figure 2.

Figure 2. PGC-1 α regulates FUNDC1 expression.

- A–C Western blotting analysis of proteins related to mitochondrial biogenesis in BATs from mice at 30°C (Normal) or following 72 h at 4°C (Cold) (A). Relative protein expression levels were normalized to Actin (B). mRNA expression levels of the indicated genes were assayed by real-time PCR and normalized to *Actb* (C). Data information: $n = 6$ biological replicates, data are represented as the mean \pm SEM. Statistical analysis was performed using two-tailed Student's *t*-test. ns: no significant difference; * $P < 0.05$; ** $P < 0.01$.
- D–F Flag-PGC-1 α was introduced into PGC-1 α knockdown brown preadipocytes for 24 h, and samples were collected for Western blotting analyses of the indicated proteins (D). Expression levels of the indicated proteins were quantified (E) (mean \pm SEM; $n = 3$). Scramble, scramble shRNA. Samples were collected for real-time PCR analysis. The expression of *Fundc1* was normalized (F). Data information: Experiments were repeated three times, and data are represented as the mean \pm SEM. Statistical analysis was performed using two-tailed Student's *t*-test. ns: no significant difference; * $P < 0.05$; ** $P < 0.01$.
- G, H Scramble and PGC-1 α knockdown preadipocytes were induced to differentiate into mature adipocytes, and samples were collected for Western blotting analyses (G) and quantification of the indicated proteins (H). Data information: Experiments were repeated three times, and data are represented as the mean \pm SEM. Statistical analysis was performed using two-tailed Student's *t*-test. ns: no significant difference; ** $P < 0.01$.

Fundc1 knockout mice expressing mito-Keima by crossing *Fundc1*^{fl/fl}/*Adiponectin*^{cre+} mice (Fig EV3D) with a mito-Keima transgenic mouse, in which the pH-dependent mitochondrion-targeted fluorescent protein mito-Keima was ubiquitously expressed. This protein is known to undergo a shift to longer-wavelength excitation when mitochondria are enclosed by acidic lysosomes, which occurs during mitophagy (Sun *et al*, 2015). When the *Fundc1*^{fl/fl}/*Adiponectin*^{cre-}/*mito-Keima*⁺ mice were exposed to cold for 3 days, the red mito-Keima signal in BAT was drastically increased (Fig 5C and D). In comparison, red mito-Keima puncta were rarely observed in BAT of *Fundc1*^{fl/fl}/*Adiponectin*^{cre+}/*mito-Keima*⁺ mice upon the identical treatment (Fig 5C and D). It is technically challenging to obtain quantitative data from fresh BAT, but the significantly reduced mito-Keima signals in *Fundc1*-depleted BAT strongly suggest that FUNDC1 was largely responsible for the increased mitophagy in cold conditions. We found that the mtDNA copy numbers were equivalent between control and *Fundc1* knockout BAT under normal unstressed conditions, and cold exposure significantly increased the mtDNA copy numbers in control mice by two-fold (Fig 5E). Unexpectedly, in the absence of FUNDC1, cold treatment did not greatly increase the mtDNA copy number, and the level of mtDNA was similar to that in controls at 30°C. The increase of total mito-keima signals (green signals) induced by cold exposure was also blunted in *Fundc1* knockout BAT (Fig 5F). The precise mechanism underlying this phenomenon warrants further investigation, and one possibility is that knockout of *Fundc1* may have a negative feedback effect on mitochondrial biogenesis. Indeed, we observed that both the PGC-1 α level and mitochondrial biogenesis are reduced in FUNDC1-deficient BAT upon cold exposure compared to the controls (Fig EV4C and D). We noticed that in our EM images, FUNDC1-deficient BAT contained a relatively high proportion of mitochondria without cristae compared to controls. Cold exposure further exacerbated the appearance of mitochondria without cristae in *Fundc1*^{fl/fl}/*Ucp1*^{cre+} BAT (Fig 5G). These data suggest that deletion of *Fundc1* results in the accumulation of functionally compromised mitochondria and much reduced mitochondrial turnover. To further substantiate this, we next performed the oxygen consumption rate (OCR) assay to measure mitochondrial functions. We found that the basal and FCCP-stimulated maximal OCRs of *Fundc1*-deficient BAT did not significantly increase upon cold exposure (Fig 5H) compared to control BAT. Despite this, mitochondrial superoxide levels were higher in *Fundc1*^{fl/fl}/*Ucp1*^{cre+} BAT than in *Fundc1*^{fl/fl}/*Ucp1*^{cre-} BAT upon cold exposure (Fig 5I). This provides further supporting evidence that mitochondria are stressed in the absence of FUNDC1. Decreased OCR, lower ATP production, and

elevated mitochondrial superoxide were also observed in *Fundc1*-deficient brown fat preadipocytes (Fig EV5A–C), although the differentiation ability of *Fundc1*-deficient brown fat preadipocytes is largely undisturbed (Fig EV5D). Collectively, these results indicate that FUNDC1-dependent mitophagy is essential for mitochondrial turnover and quality control in response to cold stress.

FUNDC1 regulates adaptive thermogenesis and contributes to cold tolerance

The increased mitochondrial biogenesis during cold acclimation creates a large capacity for oxidative phosphorylation, which can be used to generate heat through the action of the uncoupling protein UCP1. As FUNDC1-regulated mitophagy affects both mitochondrial quality and mitochondrial turnover, leading to compromised mitochondrial respiration, we speculated that the thermogenic function of BAT might also be compromised in FUNDC1-deficient mice. When *Fundc1*^{fl/fl}/*Ucp1*^{cre-} and *Fundc1*^{fl/fl}/*Ucp1*^{cre+} mice were maintained at 30°C, there was no significant difference in their baseline body temperature (Fig 6A). However, when the mice were subjected to acute cold exposure (4°C for 4 h), we observed more severe hypothermia (body temperature < 33°C) in the *Fundc1*^{fl/fl}/*Ucp1*^{cre+} mice than in the controls (Fig 6A). Furthermore, the body temperature of *Fundc1*^{fl/fl}/*Ucp1*^{cre+} mice was lower than control mice after 72-h cold acclimation, confirming the cold intolerance in *Fundc1*^{fl/fl}/*Ucp1*^{cre+} mice (Fig 6B). There was no significant difference in the weight of BAT in *Fundc1*^{fl/fl}/*Ucp1*^{cre-} and *Fundc1*^{fl/fl}/*Ucp1*^{cre+} mice in the presence or absence of cold exposure for 72 h (Fig 6C). The basal levels of *Ucp1* mRNA and protein expression are similar between *Fundc1*^{fl/fl}/*Ucp1*^{cre-} and *Fundc1*^{fl/fl}/*Ucp1*^{cre+} mice. However, the induction of *Ucp1* mRNA and protein expression upon cold exposure is increased by 31-fold and 2.3-fold, respectively, in *Fundc1*^{fl/fl}/*Ucp1*^{cre-} BAT (Fig 6D–F). This induction is blunted (12-fold and 1.2-fold) in *Fundc1*^{fl/fl}/*Ucp1*^{cre+} mice. The expression of *Ucp1* Cre alone has no effect on the cold-induced increase of UCP1 in *Ucp1*^{cre+} mice (Fig EV4E). Immunohistochemical analysis further confirmed that the expression of UCP1 protein was strongly induced in control mice, and it was blunted in the BAT of *Fundc1*^{fl/fl}/*Ucp1*^{cre+} mice upon cold exposure (Fig 6G). These results are consistent with the data above showing that mitochondrial biogenesis and quality are compromised (Fig 5), although the precise mechanism remains to be explored. Nevertheless, our data demonstrate that the protein level of FUNDC1 is regulated by PGC-1 α in an NRF1-dependent manner, and FUNDC1 is essential for mitochondrial quality control in mitochondrial biogenesis. In *Fundc1*-

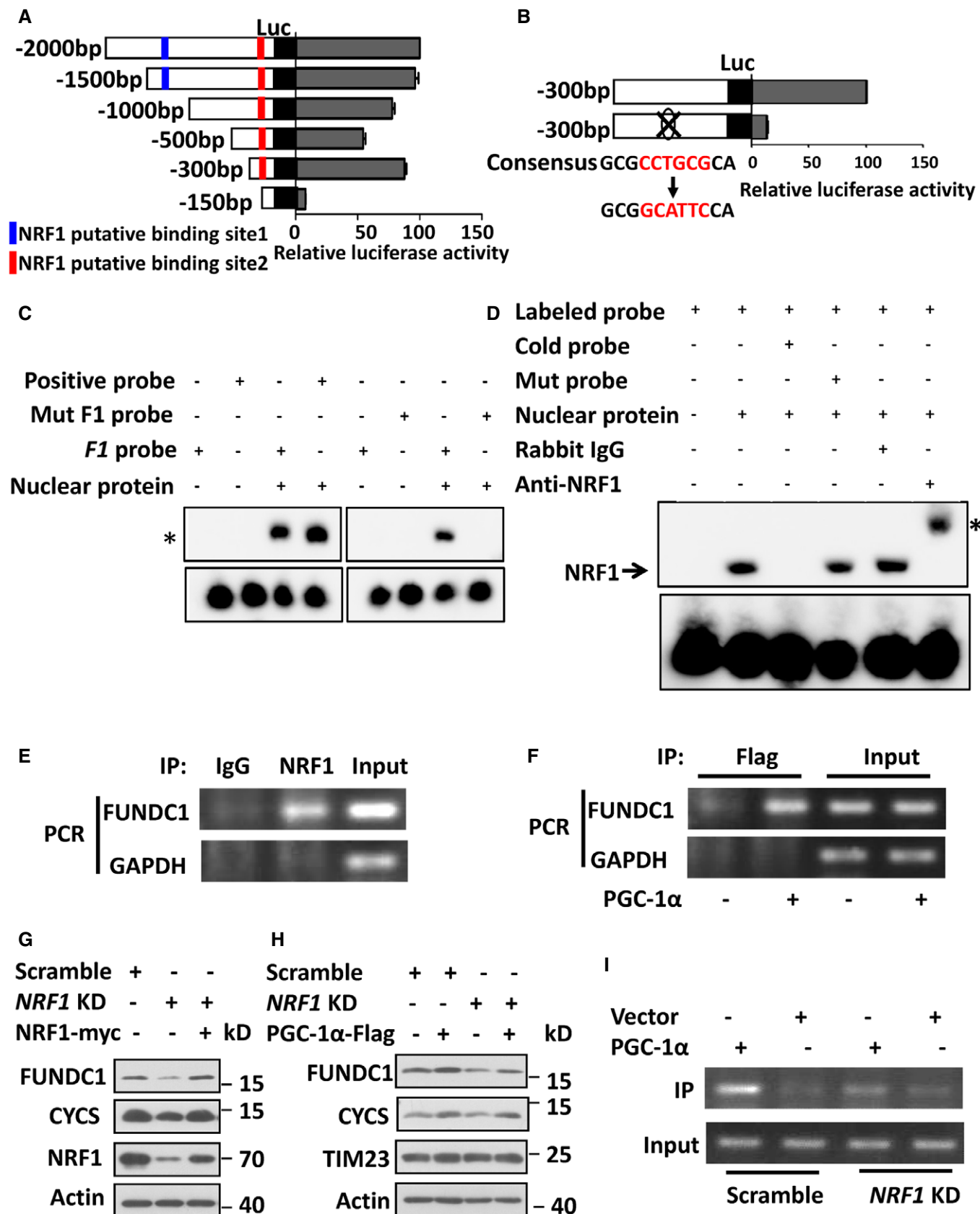


Figure 3. NRF1 transcriptionally regulates FUNDC1 expression.

- A Schematic representation of human *Fundc1* promoter deletion constructs and two putative NRF1 binding sites were marked in blue and red and the corresponding luciferase activity expressed as the activity relative to the 2,000 bp promoter. Data information: Experiments were repeated three times, and data are represented as the mean \pm SEM.
- B Luciferase activity stimulated by the human *Fundc1* promoter. The activity of *Fundc1* promoter fragments, either wild type (WT) or with a mutation in the potential NRF1 binding site, was assayed using a dual-luciferase reporter system. Data information: Experiments were repeated three times, and data are represented as the mean \pm SEM.
- C, D EMSA assay using biotinylated oligonucleotide probes containing the predicted NRF1 binding site or mutant NRF1 binding site in the promoter of *Fundc1* (*F1* probe or mut *F1* probe), the confirmed NRF1 binding site in the promoter of *VSNL1* (positive probe). The probes were incubated with HeLa nuclear extracts and then run on a gel (C). A super-shifted band (asterisk) is detected in the presence of an anti-NRF1 antibody (D). Labeled probe: biotin-labeled wild-type *Fundc1* probe; Cold probe: wild-type *Fundc1* probe; Mut probe: NRF1 binding site mutant *Fundc1* probe; asterisk indicates the super-shifted band generated with antibody to NRF1.
- E, F ChIP assay to analyze the interaction of NRF1 (E) or PGC-1 α (F) proteins with the *Fundc1* promoter.
- G NRF1-myc was introduced into NRF1 shRNA knockdown cells for 24 h, and scramble cells were used as control, and samples were collected for Western blotting with the indicated antibodies.
- H Scramble and NRF1 shRNA knockdown cells were transfected with vector and PGC-1 α -Flag for 24 h, and samples were collected for Western blotting with the indicated antibodies.
- I ChIP analysis of the interaction of PGC-1 α protein with the *Fundc1* promoter in scramble or NRF1 shRNA knockdown cells.

knockout BAT, both mitophagy and mitochondrial quality and mitochondrial biogenesis are impaired, leading to cold intolerance in mice (Fig 6H).

Discussion

Novel mechanism of coordination between mitophagy and biogenesis

It is well established that mitochondrial biogenesis is highly regulated through the PGC-1 α -NRF1 pathway. Notably, PGC-1 α senses nutritional, environmental, and developmental signals to activate NRF1 and other transcriptional factors to promote mitochondrial biogenesis and metabolic adaptations. It is widely speculated that PGC-1 α -dependent mitochondrial biogenesis should be tightly coordinated with mitophagy to maintain an optimal number of high-quality mitochondria, thus maintaining normal mitochondrial respiration, mitochondrial inheritance, and cellular functions (Kubli & Gustafsson, 2012; Palikaras & Tavernarakis, 2014). In the current study, we provide evidence to show that PGC-1 α /NRF1 transcriptionally regulate FUNDC1, a well-characterized mitophagy receptor, to enhance mitophagy, and to promote mitochondrial turnover. It is somewhat surprising that PGC-1 α and NRF1, the master regulators of mitochondrial biogenesis, directly regulate a mitophagy receptor. Thus, our results suggest a novel mechanism that coordinates mitochondrial biogenesis and mitophagy. By accelerating mitophagy during mitochondrial biogenesis, PGC-1 α /NRF1 regulation of FUNDC1-dependent mitophagy may prevent over-burdening or over-crowding of the cell with excessive mitochondria, thus maintaining normal mitochondrial and organismal physiology. Such a mechanism provides an ideal scenario for regulating mitochondrial turnover by simultaneously activating the two opposing processes to promote mitochondrial turnover and maintain the functional mitochondrial network. Enhanced turnover also accompanies FUNDC1 induction during preadipocyte differentiation. Similarly, mitophagy induced by both NIX and FUNDC1, but not Parkin, is found to reprogram the metabolic network during cardiomyocyte differentiation (Lampert *et al*, 2019). Simultaneous activation of mitophagy and mitochondrial biogenesis may also occur in many

other conditions such as physical exercise and nutrient deprivation, as it is well documented that the AMPK and mTOR pathways regulate both PGC-1 α -mediated mitochondrial biogenesis and mito(auto)phagy (Jager *et al*, 2007; Canto & Auwerx, 2009; Morita *et al*, 2013). Adipocyte AMPK is required for the adaptive response to thermogenesis and the browning program (Mottillo *et al*, 2016). We are not suggesting that PGC-1 α /NRF1 *per se* determine mitophagy, because the activity of PGC-1 α and its downstream events is mediated by an incredibly complicated network of transcriptional and post-translational modifications. Also, as we previously suggested, FUNDC1 is subjected to phosphorylation and other modifications that determine its interaction with LC3 for mitophagy. For example, an early study has shown that cold stress also induces cAMP-dependent activation of Src kinase (Fredriksson *et al*, 2000), and we have demonstrated that Src kinase phosphorylates FUNDC1 and prevents FUNDC1 interacting with LC3 (Liu *et al*, 2012). We argue that induction of FUNDC1 by PGC-1 α /NRF1 sets a new mitophagy threshold to maintain the mitochondrial network, and this is likely independent of PINK1 or Parkin activity (Liu *et al*, 2012; McWilliams *et al*, 2016; Whitworth & Pallanck, 2017; Lee *et al*, 2018; McWilliams *et al*, 2018). The regulation of mitochondrial homeostasis in mammalian systems appears to be different from that in *C. elegans*. In worms, which lack PGC-1 α , genetic depletion of DCT-1, the homolog of mammalian BNIP3 and BNIP3L/NIX, induces oxidative stress that activates SKN-1 (nuclear factor erythroid 2-related factor 2), which is completely different from NRF1, to promote mitochondrial biogenesis (Palikaras *et al*, 2015b).

Mitophagy in BAT

It was previously suggested that to maintain the higher mitochondrial content in BAT for thermogenesis, auto(mito)phagy is strongly suppressed during cold stress-induced mitochondrial biogenesis in BAT (Ferhat *et al*, 2019; Kim *et al*, 2019). Specifically, short-term cold exposure of mice resulted in a significant reduction in the expression of autophagy genes in BAT, although thermogenic gene expression was elevated (Cairo *et al*, 2016). In response to cold or β 3-AR stimulation, PKA directly phosphorylates mTOR and its binding partner, regulatory-associated protein of

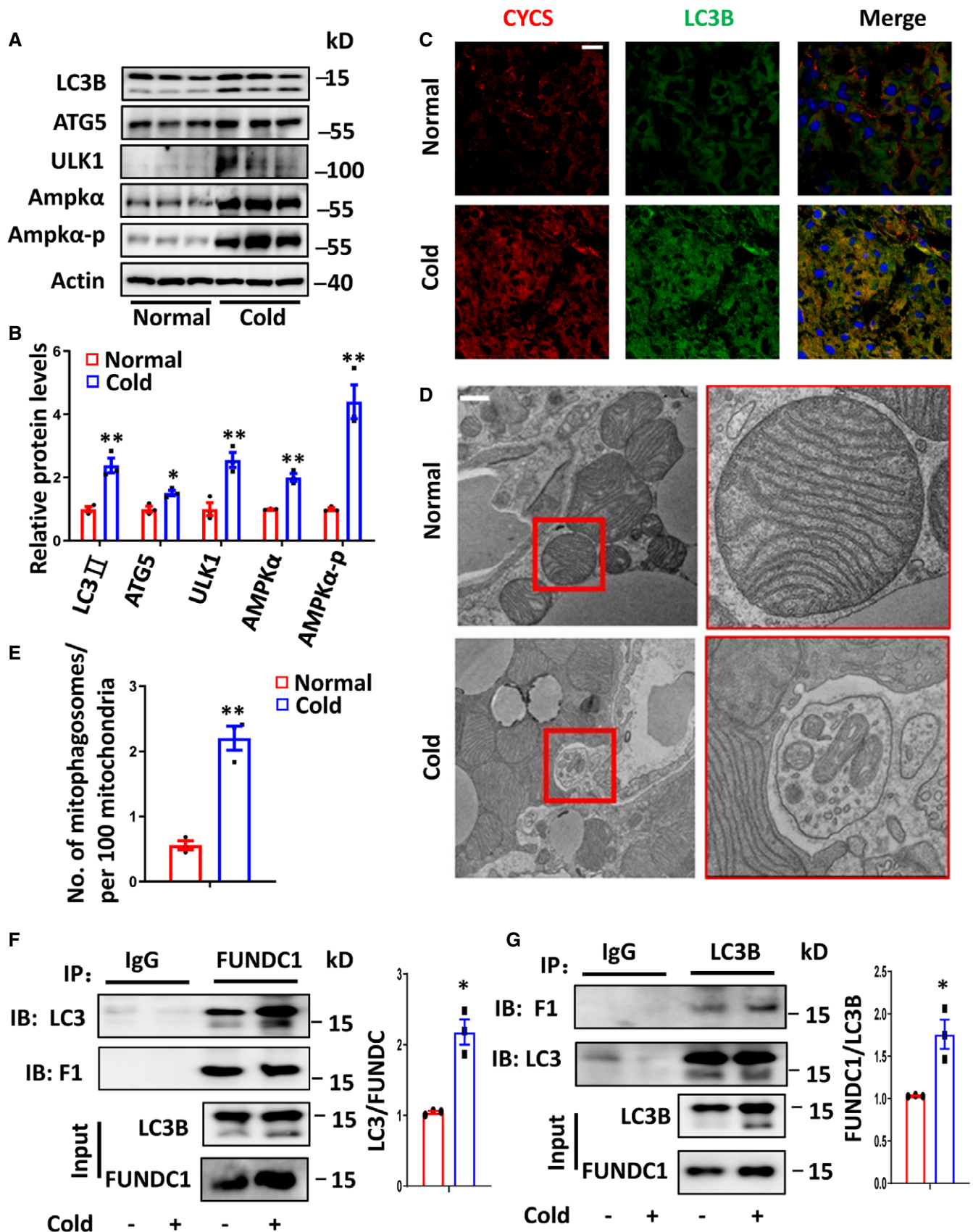


Figure 4.

Figure 4. Cold exposure induces mitophagy and the interaction between FUNDC1 and LC3.

- A, B Western blotting analyses of the levels of autophagy-related proteins in BAT from mice at the normal temperature (30°C) or at 4°C for 72 h (A). Expression of the indicated proteins was analyzed before and after 72 h cold exposure (4°C) (B). Data information: $n = 3$ biological replicates, data are represented as the mean \pm SEM. Statistical analysis was performed using two-tailed Student's *t*-test. * $P < 0.05$; ** $P < 0.01$.
- C Representative images from immunofluorescence staining of LC3B and CYCS in BAT from mice at the normal temperature (30°C) or 4°C for 72 h.
- D, E Representative transmission electron microscope (TEM) images of BAT cells isolated from mice at the normal temperature (30°C) or 4°C for 72 h. Scale bar, 1 μ m (D). The number of mitophagosomes per 100 mitochondria was counted and normalized (E). Data information: $n = 3$ biological replicates, data are represented as the mean \pm SEM. Statistical analysis was performed using two-tailed Student's *t*-test. ** $P < 0.01$.
- F, G BATs from mice exposed to normal conditions (30°C) or cold (4°C) were lysed and immunoprecipitated with antibodies against FUNDC1, LC3B, or IgG and then immunoblotted with the indicated antibodies. The ratio between immunoprecipitated LC3B to FUNDC1 or FUNDC1 to LC3B was quantified and plotted (G). Data information: Experiments were repeated three times, and data are represented as the mean \pm SEM. Statistical analysis was performed using two-tailed Student's *t*-test. * $P < 0.05$.

mTOR (RAPTOR), to stimulate the activity of mTORC1, a major regulator of autophagy (Stephan *et al*, 2009; Liu *et al*, 2016). PKA was shown to inhibit autophagy and mitophagy by modulating the expression of transcription factor genes or by inhibiting PINK1/Parkin-mediated mitophagy via phosphorylation of the mitochondrial membrane protein mitofilin (Akabane *et al*, 2016). However, these findings are in sharp contrast with recent reports showing that cold exposure or administration of beta-adrenergic agonists increases the level of autophagy and mitophagy (Lu *et al*, 2018). Our genetic, morphological, and biochemical evidence shows that physiological stimuli, such as cold, can activate mitophagy via FUNDC1, along with other ATG genes such as ATG5, LC3, and ULK1 (Fig 4A and Fig EV2F). We found that cold stress increased the expression of both FUNDC1 and LC3, induced the dephosphorylation of FUNDC1, and enhanced the FUNDC1-LC3 interaction, thus promoting mitophagy (Liu *et al*, 2012; Chen *et al*, 2014). It should be noted that it is technically challenging to measure mitophagy or mitochondrial turnover *in vivo* under physiological conditions. Early studies used protein labeling and mitochondrial protein degradation to measure mitochondrial turnover (Miwa *et al*, 2008; Gospodarska *et al*, 2015). It is now recognized that mitochondrial proteins are subjected to incredibly complex regulation at the molecular, sub-organellar, and organellar levels. Similarly, mitophagy can be mediated by a variety of mechanisms, such as those based on mitochondrial derived vesicles (MDVs),

piecemeal mitophagy, or organellar mitophagy, that degrade mitochondria partly or wholly (Sugiura *et al*, 2014). mtDNA copy number has also been used to estimate mitochondrial content. It is thus not surprising that different measurements (of mRNA levels, mitochondrial proteins, and mtDNA copy number) yield discordant results. Given the complex regulation of all mitochondrial constituents, it is important to employ integrated approaches, both *in vitro* and *in vivo*, to show that mitophagy regulates the functional network of mitochondria. Based on such a comprehensive analysis, our data suggest that PGC-1 α /NRF1 transcriptionally regulate a number of genes including *Fundc1* to dictate mitochondrial quantity, quality, and turnover, which are essential aspects of mitochondrial homeostasis.

How do enhanced mitophagy and turnover benefit BAT and organisms?

We further suggest that the coupling of mitochondrial biogenesis with FUNDC1-dependent mitophagy contributes to adaptive thermogenesis. Activating mitophagy along with mitochondrial biogenesis will maintain mitochondrial health, which is vital for thermogenesis in BAT. Good-quality mitochondria are essential for generating energy from carbohydrate in the form of pyruvate and fatty acids (for example, palmitoyl carnitine) (Cannon & Nedergaard, 2010). In unstressed conditions, mitochondrial homeostasis and

Figure 5. FUNDC1 is required for cold-induced mitophagy in mouse BAT.

- A, B BATs isolated from *Fundc1*^{fl/fl}/*Ucp1*^{cre-} (Cre-) and *Fundc1*^{fl/fl}/*Ucp1*^{cre+} (Cre+) mice at 30°C or following 72 h at 4°C were analyzed by transmission electron microscopy. Representative images are shown, scale bar, 1 μ m (A). The number of mitophagosomes per 100 mitochondria was counted and normalized (B). Data information: $n = 3$ biological replicates, data are represented as the mean \pm SEM. Statistical analysis was performed using two-way ANOVA test. ns: no significant difference; * $P < 0.05$.
- C, D Representative fluorescence images of BAT sections from *Fundc1*^{fl/fl}/*Adiponectin*^{cre-} (Cre-) and *Fundc1*^{fl/fl}/*Adiponectin*^{cre+} (Cre+) mito-Keima mice at normal conditions (30°C) or 4°C for 72 h. Scale bar, 50 μ m (C). Quantification of the ratio between red and green signals (D). Data information: $n = 6$ biological replicates, data are represented as the mean \pm SEM. Statistical analysis was performed using two-way ANOVA test. ns: no significant difference; * $P < 0.05$.
- E *Fundc*^{fl/fl}/*Ucp1*^{cre-} (Cre-) and *Fundc*^{fl/fl}/*Ucp1*^{cre+} (Cre+) mice were maintained at 30°C (Normal) or exposed to 4°C for 72 h (Cold). Mitochondrial DNA copy numbers were analyzed by real-time PCR and normalized to nuclear DNA standards. Data information: $n = 6$ biological replicates, data are represented as the mean \pm SEM. Statistical analysis was performed using two-way ANOVA test. ns: no significant difference; * $P < 0.05$.
- F The relative total mito-keima signal (green signal) in *Fundc1* deficiency and control mito-keima mice under normal condition or cold exposure were quantified and plotted. Data information: $n = 6$ biological replicates, data are represented as the mean \pm SEM. Statistical analysis was performed using two-way ANOVA test. ns: no significant difference; ** $P < 0.01$.
- G BATs isolated from *Fundc1*^{fl/fl}/*Ucp1*^{cre-} (Cre-) and *Fundc1*^{fl/fl}/*Ucp1*^{cre+} (Cre+) at 30°C or following 72 h at 4°C were analyzed by transmission electron microscopy. The percent of mitochondria without cristae is shown in the histogram. Data information: $n = 3$ biological replicates, data are represented as the mean \pm SEM. Statistical analysis was performed using two-way ANOVA test. ns: no significant difference; * $P < 0.05$.
- H, I Oxygen consumption rate (OCR) (H) and mitochondrial superoxide (I) were measured in BAT from *Fundc1*^{fl/fl}/*Ucp1*^{cre-} (Cre-) and *Fundc1*^{fl/fl}/*Ucp1*^{cre+} (Cre+) mice kept at 30°C or at 4°C for 72 h. Data information: $n = 3$ or 4 biological replicates, data are represented as the mean \pm SEM. Statistical analysis was performed using two-way ANOVA test. ns: no significant difference; * $P < 0.05$.

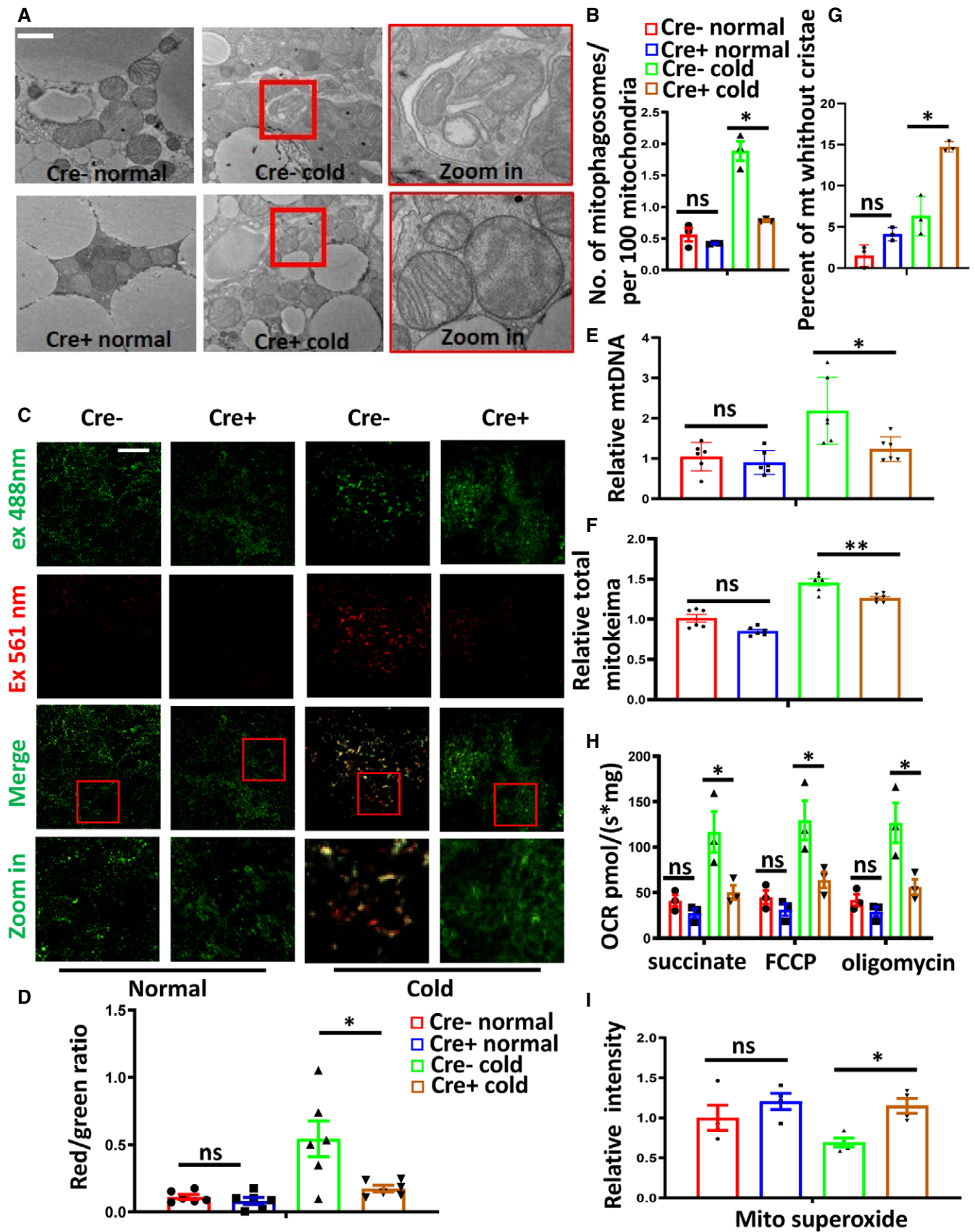


Figure 5.

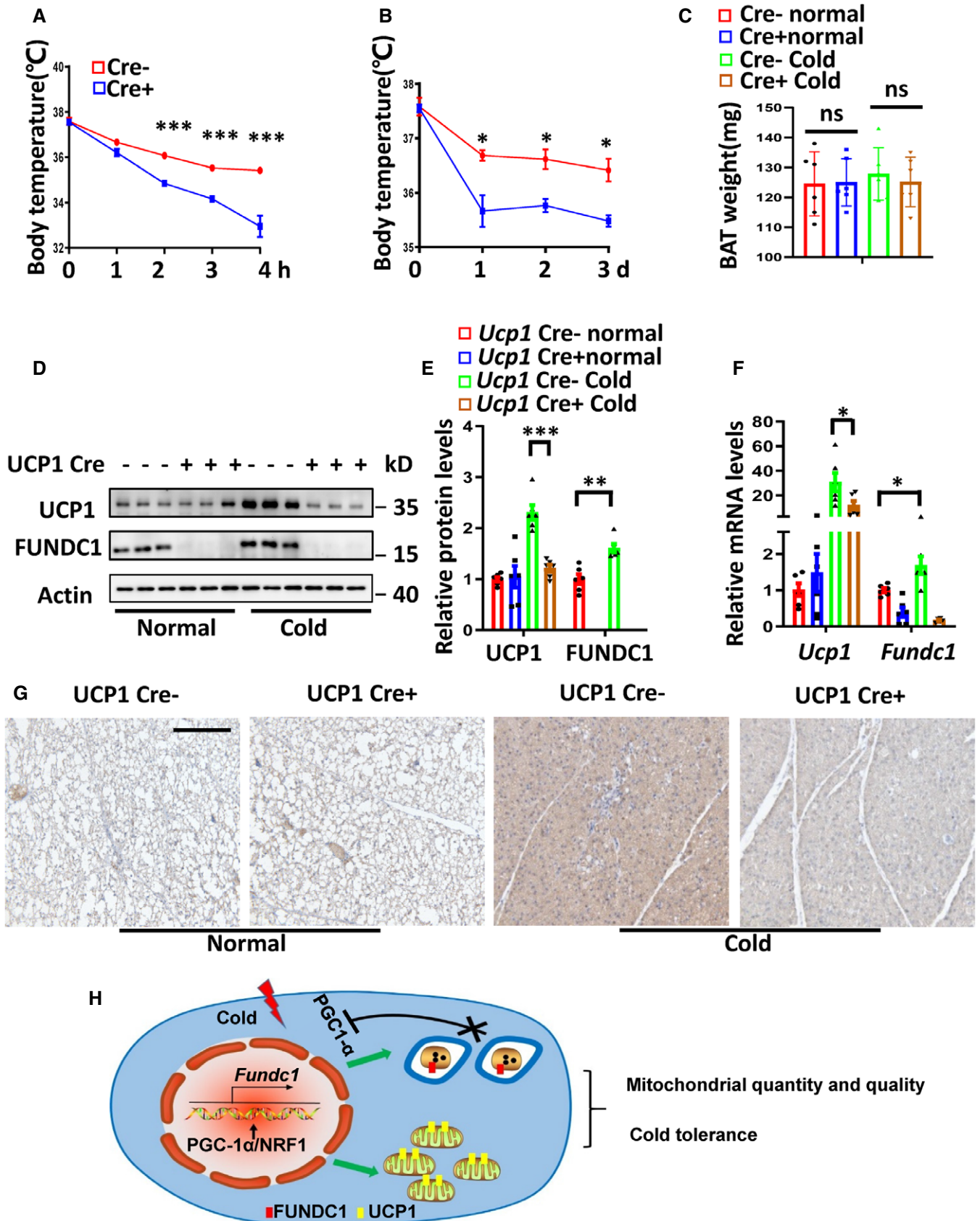


Figure 6.

Figure 6. FUNDC1 regulates adaptive thermogenesis and contributes to cold tolerance.

- A Body temperature measurements in *Fundc1^{fl/fl}/Ucp1^{cre-}* (Cre⁻) and *Fundc1^{fl/fl}/Ucp1^{cre+}* (Cre⁺) fasting male mice before and during cold exposure (4°C) for the indicated time. Data information: *n* = 6 biological replicates, data are represented as the mean ± SEM. Statistical analysis was performed using repeated measures ANOVA. ****P* < 0.001
- B, C Body temperature (B) and BAT tissue weight (C) measurements before and after 72-h cold exposure (4°C) of Cre⁻ and Cre⁺ male mice. Data information: *n* = 6 biological replicates, data are represented as the mean ± SEM. Statistical analysis was performed using repeated measures ANOVA or two-way ANOVA test. ns: no significant difference; **P* < 0.05; ****P* < 0.001.
- D–F *Fundc1^{fl/fl}/Ucp1^{cre-}* and *Fundc1^{fl/fl}/Ucp1^{cre+}* mice were exposed to 4°C for 72 h (Cold), and control mice were kept at 30°C (Normal). Western blotting analysis of BAT protein levels (D). Protein expression levels were normalized to Actin (E). Levels of mRNAs encoding *Fundc1* and *Ucp1* were measured by real-time PCR and normalized to *Actb* (F). Data information: *n* = 6 biological replicates, data are represented as the mean ± SEM. Statistical analysis was performed using two-way ANOVA test. **P* < 0.05; ***P* < 0.01; ****P* < 0.001.
- G Representative images of UCP1 immunohistochemistry of BAT sections from Cre⁻ or Cre⁺ mice in normal conditions (30°C) or following 72 h at 4°C. Scale bar, 50 μm.
- H Schematic model of PGC-1α-NRF1-FUNDC1 axis in mitochondrial quality and quantity control and adaptive thermogenesis.

mitochondrial functions, as reflected by oxygen consumption and thermogenesis, were largely maintained when *Fundc1* was deleted, likely due to compensation by yet-to-be-identified mechanisms. However, upon cold exposure, mitochondrial functions and the thermogenic gene program, including induction of the thermogenic gene *Ucp1*, were all compromised in brown fat tissue, and the BAT-specific *Fundc1* knockout mice were unable to maintain their body temperature. It is also interesting to note that under normal conditions, mtDNA copy numbers are comparable between control BAT and BAT in which *Fundc1* is specifically knocked out (Fig 5). However, in response to cold stress, the mtDNA copy numbers are lower in *Fundc1* knockout BAT, reflecting the possibility that mitochondrial biogenesis is reduced. It is likely that the absence of FUNDC1 slows down (if not completely shuts down) the removal of “old” or “exhausted” mitochondria, leading to compromised mitochondrial turnover, which exacerbates the impairments in mitochondrial functions, UCP1 expression, mitochondrial metabolism, and physiology. This mitophagy defect is further confounded with the possible feedback regulation of mitochondrial biogenesis by mitophagy, leading to compromised mitochondrial function, reduced mitochondrial number and turnover, and subsequently defective thermogenesis and cold intolerance. We have previously shown that mice lacking *Fundc1* develop more severe obesity and insulin resistance when fed a high-fat diet (HFD) (Wu *et al*, 2019), although mice with skeletal muscle-specific ablation of *Fundc1* were protected against high-fat diet-induced obesity with improved systemic insulin sensitivity and glucose tolerance despite reduced muscle mitochondrial bioenergetics (Fu *et al*, 2018). These results further demonstrate that FUNDC1-dependent mitophagy plays a critical role in cold and metabolic adaptations. In contrast, Parkin is strongly repressed when BAT is activated and its induction is blunted during BAT thermogenesis (Cairo *et al*, 2019). It is suggested that Parkin-dependent mitophagy plays a role in deacclimation (Cairo *et al*, 2019), the process by which cold-adapted mice return to a thermoneutral temperature. It is possible that FUNDC1-mediated mitophagy and Parkin-mediated mitophagy play distinct roles under different stress conditions, such as acclimation versus deacclimation, to maintain mitochondrial functions and homeostasis as previously suggested (Wei *et al*, 2015). Further work is needed to dissect the cooperative mechanisms between distinct mitophagy machineries and the crosstalk between mitophagy and mitochondrial biogenesis. Our finding that FUNDC1-dependent mitophagy is directly coupled with mitochondrial biogenesis offers a new

understanding of the molecular regulation of mitochondrial turnover and metabolism in BAT. Our results further imply that enhancing PGC-1α/NRF1 activity and FUNDC1-dependent mitochondrial turnover may be a useful therapeutic approach to fight mitochondrial, metabolic, and aging-related diseases.

Materials and Methods

Mice

Animal experiments were performed according to procedures approved by the Ethics Committee of the Institute of Zoology, Chinese Academy of Sciences. *Fundc1^{fl/fl}* mice and *Adiponectin^{cre+}* mice and C57BL/6J mice were obtained from the Model Animal Research Center of Nanjing University. *Ucp1^{cre+}* mice were obtained from Jackson Laboratories (stock #024670). The brown adipocyte-specific or adipocyte-specific *Fundc1* knockout mice were generated by crossing female *Fundc1^{fl/fl}* mice with corresponding Cre mice. Littermate male *Fundc1^{fl/fl}* Cre⁻ mice were control mice. Male mito-Keima *Fundc1* knockout mice (*Fundc1^{fl/fl}/Adiponectin^{cre+}/mito-Keima⁺*) were generated by crossing female *Fundc1^{fl/fl}/Adiponectin^{cre+}* with male *Fundc1^{fl/y}/Adiponectin^{cre-}/mito-Keima⁺* mice. All mice were housed at 30°C with a 12-h light/12-h dark cycle and given free access to water and food. The cold test experiment was performed by housing mice at 4°C for the indicated time, then measuring rectal body temperature.

Indirect calorimetry

Energy expenditure was evaluated by measuring oxygen consumption with a TSE Systems Indirect Gas Calorimetry system. The difference in CO₂ and O₂ concentrations was measured with CO₂ and O₂ sensors, and the respiratory exchange ratio (RER) was calculated using the VCO₂/VO₂ ratio. Mice were housed individually and maintained at 30°C under a 12-h light/12-h dark cycle. Food and water were available *ad libitum*.

Cell culture and transfection

Interscapular brown fat pads from fetal wild-type or *Fundc1* germline knockout mice were isolated rapidly and minced. The fat mince was digested with 1.5 mg/ml Collagenase A at 37°C with constant

agitation for 40 min. Five milliliter DMEM medium supplemented with 20% FBS was added, and the cells were pelleted by centrifugation at 500 g for 10 min. Then, the preadipocyte suspension was filtered through a 100 µm filter, resuspended, and plated in a sterile Petri dish containing DMEM medium supplemented with 20% FBS. Preadipocytes were immortalized by infection with the retroviral vector pBabe encoding SV40 large T antigen and then selected with puromycin (1 µg/ml) for 7 days. Preadipocytes were grown to confluence in culture medium supplemented with 20 nM insulin and 1 nM T3 (differentiation medium; day 0). Brown adipocyte differentiation was induced by treating confluent cells for 48 h in differentiation medium further supplemented with 0.5 mM isobutylmethylxanthine, 0.5 mM dexamethasone, and 0.125 mM indomethacin. After this induction period (day 2), the medium was washed out and cells were incubated for a further 5 days in differentiation medium, which was changed every 2 days. Full differentiation was achieved after 5 days. PGC-1 α and PGC-1 β knockdown cell lines were generated using retroviral-mediated expression of shRNA specific for PGC-1 α and PGC-1 β and scramble shRNA as a control. Infected cells were selected with puromycin (1 µg/ml) for 7 days. For adenoviral infections, preadipocytes were transduced overnight with GFP or PGC-1 α expression virus and cells were harvested after 48 h. All cells were grown in DMEM with 10% FBS and 1% penicillin–streptomycin at 37°C under 5% CO₂. The target sequence in PGC-1 α for RNA interference is 5'-GACGGATTGCCCTCATTTG; the target sequence in PGC-1 β is 5'-CCTTCCAATATGTTTACGTTT; the target sequence in NRF1 is 5'-CACATGGCTACCATAGAAG; and the scramble RNA interference sequence is 5'-GACATTTGTAACGG GATTTC. Primers for shRNA were cloned into pSuper-retro-puro or pSicoR vectors. ShRNA expression viruses were packaged by transfecting the vector into HEK-293T cells. To establish stable cell lines, cells were transduced with the corresponding vectors and selected with puromycin or sorted by flow cytometry.

Antibodies and reagents

The following antibodies were used: anti-TIM23 monoclonal antibody, anti-Cytochrome *c* monoclonal antibody (BD Biosciences); anti-PINK1 monoclonal antibody (Abgent), anti-LC3B polyclonal antibody (MBL), anti-Actin monoclonal antibody, anti-UCP1 polyclonal antibody, anti-Flag monoclonal antibody (Sigma); anti-VDAC1 monoclonal antibody (Abcam); anti-NRF1 polyclonal antibody (Santa Cruz); anti-PGC-1 α polyclonal and monoclonal antibody (Merck); anti-PGC-1 β polyclonal antibody (Proteintech); anti-PARKIN polyclonal antibody, anti-TFAM polyclonal antibody, anti-ATG5 polyclonal antibody, anti-ULK1 polyclonal antibody; and anti-HSP60 polyclonal antibody, anti-NIX polyclonal (CST). Polyclonal antibodies against FUNDC1 were generated by immunizing rabbits with recombinant FUNDC1 (delta TM domain) protein produced in *Escherichia coli* using PGEX4T1 expression vector. The fluorescent secondary antibodies were goat anti-mouse IgG Cy3 and goat anti-rabbit FITC IgG (DAKO).

The following reagents were used: TMRE, Mito-SOX, EMSA/Gel Shift kit (Thermo Fisher); ATP detection kit, chromatin immunoprecipitation (CHIP) Assay kit (Beyotime); Dual-Luciferase Reporter (DLR™) Assay System (Promega); and Tissue DNA extraction kit (Tiagene).

Real-time PCR analysis

RNA was prepared using TRIzol Reagent (Invitrogen). The cDNA was synthesized using a cDNA synthesis kit (Takara). Real-time PCR was carried out using a One Step qRT-PCR (Probe) Kit (Tiangen) and a CFX96 real-time PCR detection system (Bio-Rad). Relative abundance of mRNA was calculated after normalization to *Actb* expression.

For real-time PCR, primers were as follows:

Fundc1	5'-AGACACCACTGGTGAATCGAG (F)
	5'-CCTTCTGGAATAAAAAATCCTGCAC (R)
PARKIN	5'-TGTCCTCACTCCCTGATTAAG (F)
	5'-ACAGCACACCTCCCATTTG (R)
PINK1	5'-CGACAACATCCTTGTGGAGTGG (F)
	5'-CATTGCCACCACGCTCTACT (R)
TFAM	5'-GAGGCAAAGGATGATTCCGGCTC (F)
	5'-CGAATCCTATCATCTTTAGCAAGC (R)
PGC-1 α	5'-CCCTGCCATTGTTAAGACC (F)
	5'-TGCTGCTGTCTCTGTTTTC (R)
NRF1	5'-GGCAACAGTAGCCACATTGGCT (F)
	5'-GTCTGGATGGTCATTTACCCG (R)
Tim23	5'-GGTGCAGAAGATGACCTCAACAC (F)
	5'-GCATAGAGACTGGTGAAGTGCAG (R)
HSP60	5'-TGCTCATCGGAAGCCATTGGTC (F)
	5'-TTGACTGCCACAACCTGAAGACC (R)
VDAC1	5'-AGTGACCCAGAGCAACTTCGCA (F)
	5'-CAGGCGAGATTGACAGCACTCT (R)
Nix	5'-GCATGAGGAAGAGTGGAGCCAT (F)
	5'-AAGGTGTGCTCAGTCGTTTTCCA (R)
UCP1	5'-GCTTTGCCTCACTCAGGATTGG (F)
	5'-CCAATGAACACTGCCACACCTC (R)
CYCS	5'-GAGGCAAGCATAAAGACTGGACC (F)
	5'-ACTCCATCAGGATCCTCTCC (R)
LC3B	5'-GTCCTGGACAAGACCAAGTTCC (F)
	5'-CCATTCACCAGGAGGAAGAAGG (R)
Atg5	5'-CTTGATCAAGTTCAGCTCTTCC (F)
	5'-AAGTGAAGCTCAACCGCATCCT (R)
ULK1	5'-GCAGCAAAGACTCCTGTGACAC (F)
	5'-CCACTACACAGCAGGCTATCAG (R)
Actb	5'-GGCGCTTTTGACTCAGGATT (F)
	5'-GGGATGTTTGCTCCAACCAA (R)

Transmission electron microscopy (TEM)

BAT was freshly isolated from the indicated mice and then cut into small pieces (1 mm³) in 2.5% glutaraldehyde. The samples were fixed at 37°C in 2.5% glutaraldehyde for 1 h, then dehydrated in a graded series of ethanol, and embedded in Epon 812 resin. Ultrathin sections were cut and observed under a Tecnai G2 F20 TWIN TMP EM. The electron micrographs were captured at 5,000 \times magnification, and the numbers of mitochondria were counted and normalized. The data are presented

as number of mitophagosomes per 100 mitochondria. The numbers of mitochondria without cristae and normal mitochondria were counted, and the percentage of mitochondria without cristae was calculated. For each animal, at least 20 micrographs were captured.

SDS-PAGE and Western blotting

Cells or homogenized tissue were lysed in lysis buffer (20 mM Tris, pH 7.4, 2 mM EGTA, 1% NP-40, protease inhibitors). The total protein concentration was determined by the Bradford method. Equivalent protein quantities were subjected to SDS-PAGE and transferred to nitrocellulose membranes. Membranes were probed with the corresponding primary antibodies, followed by the appropriate HRP-conjugated secondary antibodies (KPL). Immunoreactive bands were visualized with a chemiluminescence kit (Pierce) and quantified by Image J software.

Mito-superoxide measurement

Cells were harvested, resuspended in PBS containing 5 μ M mitochondrial superoxide indicator Mito-SOX, and stained for 30 min at 37°C in the dark. The cells were then washed with ice-cold PBS twice and analyzed with flow cytometry.

ATP measurement

ATP levels in cultured cells and fresh tissues were measured using an ATP determination kit following the manufacturer's protocol (Beyotime Biotechnology). Briefly, 10^6 cells or 10 mg homogenized fresh tissues were lysed. After centrifugation at 13,000 g for 15 min, the supernatant was collected and the protein concentration was determined. Equivalent amounts of supernatants were used for measurement, and luminescence was recorded by an illuminometer. The relative ATP level was normalized by calculating the ratios between the luminescence intensities of the corresponding proteins with control samples.

Measurement of mitochondrial oxygen consumption rate

Freshly isolated BAT was weighed, and 5 mg of tissue was homogenized in respiration medium B (0.5 mM EGTA, 3 mM $\text{MgCl}_2 \cdot 6\text{H}_2\text{O}$, 20 mM taurine, 10 mM KH_2PO_4 , 20 mM HEPES, 0.1% BSA, 60 mM potassium lactobionate, 110 mM mannitol, 0.3 mM dithiothreitol, pH 7.1) with succinate as the substrate. Uncoupled and maximal OCR were determined using oligomycin (10 μ M) and FCCP (10 μ M). For measurement of OCR in cells, the cells were harvested and resuspended in assay buffer (50 mM KCl, 4 mM KH_2PO_4 , 5 mM HEPES, 1 mM EGTA, 4% BSA, 10 mM pyruvate, 5 mM malate). Uncoupled and maximal OCR were determined using oligomycin (10 μ M) and FCCP (10 μ M). Antimycin A was used to inhibit Complex III-related respiration. OCR in homogenized tissue and cells was determined using an Oxygraph 2K. The OCR was finally standardized to the cell number or tissue weight.

Measurement of mitochondrial DNA copy number

Total DNA was extracted from freshly isolated tissues with a tissue DNA extraction kit. Ten nanogram DNA from each sample was used

to quantify the mitochondrial DNA copy number by real-time PCR. The mtDNA quantity was corrected by simultaneous measurement of nuclear DNA standards. The primers were published previously (Vernia *et al*, 2014). Primers for mtDNA were CytBF 5'-ATTCCTT-CATGTCGGACGAG, CytBR 5'-ACTGAGAAGCCCCCTCAAAT, and the primers for nuclear DNA were H19F 5'-GTCCACGAGACCAAT-GACTG, H19R 5'-GTACCCACCTGTCGTCC.

Mito-Keima assay

For mito-Keima assays in tissues, brown adipose tissues were rapidly isolated and cut into small pieces (100 mm^3). The tissue pieces were placed in confocal dishes, and images were captured with a Nikon confocal microscope. Mito-Keima fluorescence was captured in two channels via two sequential excitations (488-nm, green; 561-nm, red) using the same 620-nm emission. The mito-Keima fluorescent signal from 561-nm laser excitation was depicted in red, and the signal from 488-nm laser excitation was in green. The fluorescence intensities of 561-nm and 488-nm excited Mito-Keima signals were measured by Image J software, and the 561-nm:488-nm ratios were calculated.

Immunohistochemistry

Fresh fat tissues were rapidly isolated, fixed with 4% paraformaldehyde in phosphate-buffered saline (PBS), and embedded in paraffin. The fixed fat samples were sectioned at thicknesses of 5–10 μ m. The samples were then stained with the indicated primary antibody overnight and with the secondary antibody for 30 min at room temperature (RT). Images were captured by a Vectra Automated Quantitative Pathology Imaging System.

Electrophoretic mobility shift assay

The following biotin-labeled NRF1 oligonucleotides and NRF1 binding domain mutant oligonucleotides were used. F1 5'-TTT CGCGCTGCGCAGAAGG (F) and 5'-GCCTTCTGCGCAGCGCGAA. (R); Mut F1 5'-TTTCGCGCATTCCAGAAGG (F) and 5'-GCCTT CTGGAATGCCGCGAA (R). The positive control oligonucleotides were TCGCGCGCTGCGCATCCAG (F) and 5'-GCTGGATGCGCAG GCGCGG (R). The competitor-mutant oligonucleotides were 5'-TTTCGCGCATTCCAGAAGG (F) and 5'-GCCTTCTGGAATGCCGCG GAA (R). Equal amounts of the forward and reverse oligonucleotides were annealed. DNA binding was performed at RT for 20 min in a mixture containing 10 μ g of nuclear extract, 5 \times gel shift binding buffer, and 1 μ l of biotin-labeled probe. In the competition experiment, 100 \times unlabeled double-stranded oligonucleotides were used and incubated with nuclear extract and binding buffer for 10 min following addition of biotin-labeled probe for 20 min at RT. In super-shift assays, the NRF1 antibody was also incubated with the reaction mixture at RT for 30 min before the addition of the biotin-labeled probe. Finally, the reaction mixtures were mixed with 10 \times loading buffer and analyzed on a 4% DNA retardation gel at 10 V/cm on ice for 1.5 h.

Chromatin immunoprecipitation

Proteins were cross-linked to DNA by incubating 5×10^6 cells with 1% formaldehyde for 10 min at 37°C. The cell pellets were resuspended in 200 μ l SDS lysis buffer followed by DNA sonication for a total of five times (10 s each time at 30% of maximal power) using an Ultrasonic Processor. Immunocomplexes were captured from the rest of the lysates with 2 μ g of the corresponding antibodies. PCR was performed using 1% of the immunoprecipitate. Primers for the *Fundc1* promoter were: 5'-GAAGGCAACGGACTACAA (F), 5'-GATG-GAAGTCTATGGTCTCTT (R). The following PCR program was used: 95°C for 5 min followed by 35 cycles of 95°C for 30 s, 56°C for 30 s, 72°C for 30 s, and finally 72°C for 10 min.

Statistical analysis

Statistical analysis was performed using Student's *t*-test or ANOVA test. $P < 0.05$ was considered statistically significant. * $P < 0.05$, ** $P < 0.01$, and *** $P < 0.001$ versus the corresponding controls are indicated. All statistical calculations were performed with GraphPad Prism and SPSS software.

Data availability

This study includes no data deposited in external repositories.

Expanded View for this article is available online.

Acknowledgements

We wish to thank Professor Shengcai Lin from Xiamen University and Professor Xiangdong Fu from UCSD for their critical comments on the manuscript and also Isabel Hanson for her English editing. We thank Dr. Yiguo Wang from Tsinghua University for providing the PGC-1 α and control GFP adenoviruses. We wish to thank Dr. Wanzhu Jin and Dr. Hanlin Zhang from the Institute of Zoology for their assistance with mouse temperature measurements. We wish to thank Dr. Guo-peng Wang from the Core Facilities at the School of Life Sciences, Peking University, as well as Yinzi Ma and Pengyan Xia from the Electron Microscope Center, State Key Laboratory of Membrane Biology, Institute of Zoology, for their assistance with transmission electron microscopy work. This research was supported by the National Natural Science Foundation of China (31790404, 91849201, 91854105, 31671446, 31520203904) and Grants 2019YFA0508601 and 2016YFA0500201 from the Ministry of Science and Technology of China.

Author contributions

LL and QC designed the experiments. LL, QC, XL, and ZY wrote and revised the manuscript. LL performed most of the experiments with the help of YL, JW, DZ, HW, WL, HW, NT, YF, and YL. XP provided mito-keima mice. XW and JW provided technical support for the project. All authors provided intellectual input and read the manuscript.

Conflict of interest

The authors declare that they have no conflict of interest.

References

- Akabane S, Uno M, Tani N, Shimazaki S, Ebara N, Kato H, Kosako H, Oka T (2016) PKA regulates PINK1 stability and parkin recruitment to damaged mitochondria through phosphorylation of MIC60. *Mol Cell* 62: 371–384
- Altshuler-Keylin S, Kajimura S (2017) Mitochondrial homeostasis in adipose tissue remodeling. *Sci Signal* 10: eaai9248
- Anderson RM, Barger JL, Edwards MG, Braun KH, O'Connor CE, Prolla TA, Weindruch R (2008) Dynamic regulation of PGC-1 α localization and turnover implicates mitochondrial adaptation in calorie restriction and the stress response. *Aging Cell* 7: 101–111
- Aquilano K, Vigilanza P, Baldelli S, Pagliei B, Rotilio G, Ciriolo MR (2010) Peroxisome proliferator-activated receptor gamma co-activator 1 α (PGC-1 α) and sirtuin 1 (SIRT1) reside in mitochondria: possible direct function in mitochondrial biogenesis. *J Biol Chem* 285: 21590–21599
- Artal-Sanz M, Tavernarakis N (2009) Prohibitin couples diapause signalling to mitochondrial metabolism during ageing in *C. elegans*. *Nature* 461: 793–797
- Ashrafi G, Schwarz TL (2013) The pathways of mitophagy for quality control and clearance of mitochondria. *Cell Death Differ* 20: 31–42
- Barbera MJ, Schluter A, Pedraza N, Iglesias R, Villarroya F, Giralt M (2001) Peroxisome proliferator-activated receptor alpha activates transcription of the brown fat uncoupling protein-1 gene. A link between regulation of the thermogenic and lipid oxidation pathways in the brown fat cell. *J Biol Chem* 276: 1486–1493
- Bhujabal Z, Birgisdottir AB, Sjøttem E, Brenne HB, Overvatn A, Habisov S, Kirkin V, Lamark T, Johansen T (2017) FKBP8 recruits LC3A to mediate Parkin-independent mitophagy. *EMBO Rep* 18: 947–961
- Birkenfeld AL, Lee HY, Guebre-Egziabher F, Alves TC, Jurczak MJ, Jornayvaz FR, Zhang D, Hsiao JJ, Martin-Montalvo A, Fischer-Rosinsky A et al (2011) Deletion of the mammalian INDY homolog mimics aspects of dietary restriction and protects against adiposity and insulin resistance in mice. *Cell Metab* 14: 184–195
- Cairo M, Villarroya J, Cereijo R, Campderros L, Giralt M, Villarroya F (2016) Thermogenic activation represses autophagy in brown adipose tissue. *Int J Obes (Lond)* 40: 1591–1599
- Cairo M, Campderros L, Gavalda-Navarro A, Cereijo R, Delgado-Angles A, Quesada-Lopez T, Giralt M, Villarroya J, Villarroya F (2019) Parkin controls brown adipose tissue plasticity in response to adaptive thermogenesis. *EMBO Rep* 20: e46832
- Cannon B, Nedergaard J (2004) Brown adipose tissue: function and physiological significance. *Physiol Rev* 84: 277–359
- Cannon B, Nedergaard J (2010) Metabolic consequences of the presence or absence of the thermogenic capacity of brown adipose tissue in mice (and probably in humans). *Int J Obes (Lond)* 34(Suppl 1): S7–S16
- Canto C, Auwerx J (2009) PGC-1 α , SIRT1 and AMPK, an energy sensing network that controls energy expenditure. *Curr Opin Lipidol* 20: 98–105
- Chen CT, Hsu SH, Wei YH (2012) Mitochondrial bioenergetic function and metabolic plasticity in stem cell differentiation and cellular reprogramming. *Biochim Biophys Acta* 1820: 571–576
- Chen G, Han Z, Feng D, Chen Y, Chen L, Wu H, Huang L, Zhou C, Cai X, Fu C et al (2014) A regulatory signaling loop comprising the PGAM5 phosphatase and CK2 controls receptor-mediated mitophagy. *Mol Cell* 54: 362–377

- Corti O, Brice A (2013) Mitochondrial quality control turns out to be the principal suspect in parkin and PINK1-related autosomal recessive Parkinson's disease. *Curr Opin Neurobiol* 23: 100–108
- Dagda RK, Zhu J, Kulich SM, Chu CT (2008) Mitochondrially localized ERK2 regulates mitophagy and autophagic cell stress: implications for Parkinson's disease. *Autophagy* 4: 770–782
- del Mar Gonzalez-Barroso G-B, Pecqueur C, Gelly C, Sanchis D, Alves-Guerra MC, Bouillaud F, Ricquier D, Cassard-Doulcier AM (2000) Transcriptional activation of the human ucp1 gene in a rodent cell line. Synergism of retinoids, isoproterenol, and thiazolidinedione is mediated by a multipartite response element. *J Biol Chem* 275: 31722–31732
- Diaz F, Moraes CT (2008) Mitochondrial biogenesis and turnover. *Cell Calcium* 44: 24–35
- Dominy JE, Puigserver P (2013) Mitochondrial biogenesis through activation of nuclear signaling proteins. *Cold Spring Harb Perspect Biol* 5: a015008
- Dorn 2nd GW (2010) Mitochondrial pruning by Nix and BNIP3: an essential function for cardiac-expressed death factors. *J Cardiovasc Transl Res* 3: 374–383
- Dorn 2nd GW, Vega RB, Kelly DP (2015) Mitochondrial biogenesis and dynamics in the developing and diseased heart. *Genes Dev* 29: 1981–1991
- Drake JC, Laker RC, Wilson RJ, Zhang M, Yan Z (2019) Exercise-induced mitophagy in skeletal muscle occurs in the absence of stabilization of Pink1 on mitochondria. *Cell Cycle* 18: 1–6
- Fan W, Evans R (2015) PPARs and ERRs: molecular mediators of mitochondrial metabolism. *Curr Opin Cell Biol* 33: 49–54
- Ferhat M, Funai K, Boudina S (2019) Autophagy in adipose tissue physiology and pathophysiology. *Antioxid Redox Signal* 31: 487–501
- Fernandez-Marcos PJ, Auwerx J (2011) Regulation of PGC-1alpha, a nodal regulator of mitochondrial biogenesis. *Am J Clin Nutr* 93: 884S–890
- Fredriksson JM, Lindquist JM, Bronnikov GE, Nedergaard J (2000) Norepinephrine induces vascular endothelial growth factor gene expression in brown adipocytes through a beta-adrenoreceptor/cAMP/protein kinase A pathway involving Src but independently of Erk1/2. *J Biol Chem* 275: 13802–13811
- Fu J, Zhang J, Jin F, Patchefsky J, Braunewell KH, Klein-Szanto AJ (2009) Promoter regulation of the visinin-like subfamily of neuronal calcium sensor proteins by nuclear respiratory factor-1. *J Biol Chem* 284: 27577–27586
- Fu T, Xu Z, Liu L, Guo Q, Wu H, Liang X, Zhou D, Xiao L, Liu L, Liu Y et al (2018) Mitophagy directs muscle-adipose crosstalk to alleviate dietary obesity. *Cell Rep* 23: 1357–1372
- Gospodarska E, Nowialis P, Kozak LP (2015) Mitochondrial turnover: a phenotype distinguishing brown adipocytes from interscapular brown adipose tissue and white adipose tissue. *J Biol Chem* 290: 8243–8255
- Gottlieb RA, Carreira RS (2010) Autophagy in health and disease. 5. Mitophagy as a way of life. *Am J Physiol Cell Physiol* 299: C203–C210
- Gottlieb RA, Gustafsson AB (2011) Mitochondrial turnover in the heart. *Biochim Biophys Acta* 1813: 1295–1301
- Gottlieb RA, Pourpirali S (2016) Lost in translation: miRNAs and mRNAs in ischemic preconditioning and ischemia/reperfusion injury. *J Mol Cell Cardiol* 95: 70–77
- Gottlieb RA, Thomas A (2017) Mitophagy and mitochondrial quality control mechanisms in the heart. *Curr Pathobiol Rep* 5: 161–169
- Greene AW, Grenier K, Aguilera MA, Muise S, Farazifard R, Haque ME, McBride HM, Park DS, Fon EA (2012) Mitochondrial processing peptidase regulates PINK1 processing, import and Parkin recruitment. *EMBO Rep* 13: 378–385
- He C, Klionsky DJ (2009) Regulation mechanisms and signaling pathways of autophagy. *Annu Rev Genet* 43: 67–93
- Hickson-Bick DL, Jones C, Buja LM (2008) Stimulation of mitochondrial biogenesis and autophagy by lipopolysaccharide in the neonatal rat cardiomyocyte protects against programmed cell death. *J Mol Cell Cardiol* 44: 411–418
- Huo L, Scarpulla RC (2001) Mitochondrial DNA instability and peri-implantation lethality associated with targeted disruption of nuclear respiratory factor 1 in mice. *Mol Cell Biol* 21: 644–654
- Jacobsson A, Cannon B, Nedergaard J (1987) Physiological activation of brown adipose tissue destabilizes thermogenin mRNA. *FEBS Lett* 224: 353–356
- Jager S, Handschin C, St-Pierre J, Spiegelman BM (2007) AMP-activated protein kinase (AMPK) action in skeletal muscle via direct phosphorylation of PGC-1alpha. *Proc Natl Acad Sci USA* 104: 12017–12022
- Jin SM, Lazarou M, Wang C, Kane LA, Narendra DP, Youle RJ (2010) Mitochondrial membrane potential regulates PINK1 import and proteolytic destabilization by PARL. *J Cell Biol* 191: 933–942
- Kabeya Y, Mizushima N, Ueno T, Yamamoto A, Kirisako T, Noda T, Kominami E, Ohsumi Y, Yoshimori T (2000) LC3, a mammalian homologue of yeast Apg8p, is localized in autophagosome membranes after processing. *EMBO J* 19: 5720–5728
- Kaeberlein M (2010) Lessons on longevity from budding yeast. *Nature* 464: 513–519
- Kelly DP, Scarpulla RC (2004) Transcriptional regulatory circuits controlling mitochondrial biogenesis and function. *Genes Dev* 18: 357–368
- Kim D, Kim JH, Kang YH, Kim JS, Yun SC, Kang SW, Song Y (2019) Suppression of brown adipocyte autophagy improves energy metabolism by regulating mitochondrial turnover. *Int J Mol Sci* 20: 3520
- Kong X, Banks A, Liu T, Kazak L, Rao RR, Cohen P, Wang X, Yu S, Lo JC, Tseng YH et al (2014) IRF4 is a key thermogenic transcriptional partner of PGC-1alpha. *Cell* 158: 69–83
- Kubli DA, Gustafsson AB (2012) Mitochondria and mitophagy: the yin and yang of cell death control. *Circ Res* 111: 1208–1221
- Kundu M, Lindsten T, Yang CY, Wu JM, Zhao FP, Zhang J, Selak MA, Ney PA, Thompson CB (2008) Ulk1 plays a critical role in the autophagic clearance of mitochondria and ribosomes during reticulocyte maturation. *Blood* 112: 1493–1502
- Laker RC, Drake JC, Wilson RJ, Lira VA, Lewellen BM, Ryall KA, Fisher CC, Zhang M, Saucerman JJ, Goodyear LJ et al (2017) Ampk phosphorylation of Ulk1 is required for targeting of mitochondria to lysosomes in exercise-induced mitophagy. *Nat Commun* 8: 548
- Lampert MA, Orogo AM, Najor RH, Hammerling BC, Leon LJ, Wang BJ, Kim T, Sussman MA, Gustafsson AB (2019) BNIP3L/NIX and FUNDC1-mediated mitophagy is required for mitochondrial network remodeling during cardiac progenitor cell differentiation. *Autophagy* 15: 1182–1198
- Lee JJ, Sanchez-Martinez A, Zarate AM, Beninca C, Mayor U, Clague MJ, Whitworth AJ (2018) Basal mitophagy is widespread in *Drosophila* but minimally affected by loss of Pink1 or parkin. *J Cell Biol* 217: 1613–1622
- Leone TC, Lehman JJ, Finck BN, Schaeffer PJ, Wende AR, Boudina S, Courtois M, Wozniak DF, Sambandam N, Bernal-Mizrachi C et al (2005) PGC-1alpha deficiency causes multi-system energy metabolic derangements: muscle dysfunction, abnormal weight control and hepatic steatosis. *PLoS Biol* 3: e101
- Li W, Li Y, Siraj S, Jin H, Fan Y, Yang X, Huang X, Wang X, Wang J, Liu L et al (2019) FUN14 domain-containing 1-mediated mitophagy suppresses hepatocarcinogenesis by inhibition of inflammasome activation in mice. *Hepatology* 69: 604–621

- Lin J, Wu PH, Tarr PT, Lindenberg KS, St-Pierre J, Zhang CY, Mootha VK, Jager S, Vianna CR, Reznick RM et al (2004) Defects in adaptive energy metabolism with CNS-linked hyperactivity in PGC-1 α null mice. *Cell* 119: 121–135
- Liu L, Feng D, Chen G, Chen M, Zheng Q, Song P, Ma Q, Zhu C, Wang R, Qi W et al (2012) Mitochondrial outer-membrane protein FUNDC1 mediates hypoxia-induced mitophagy in mammalian cells. *Nat Cell Biol* 14: 177–185
- Liu L, Sakakibara K, Chen Q, Okamoto K (2014) Receptor-mediated mitophagy in yeast and mammalian systems. *Cell Res* 24: 787–795
- Liu D, Bordicchia M, Zhang C, Fang H, Wei W, Li JL, Guilherme A, Guntur K, Czech MP, Collins S (2016) Activation of mTORC1 is essential for beta-adrenergic stimulation of adipose browning. *J Clin Invest* 126: 1704–1716
- Lowell BB, Spiegelman BM (2000) Towards a molecular understanding of adaptive thermogenesis. *Nature* 404: 652–660
- Lu Y, Fujioka H, Joshi D, Li Q, Sangwung P, Hsieh P, Zhu J, Torio J, Sweet D, Wang L et al (2018) Mitophagy is required for brown adipose tissue mitochondrial homeostasis during cold challenge. *Sci Rep* 8: 8251
- Manfredi LH, Ang J, Peker N, Dagda RK, McFarlane C (2019) G protein-coupled receptor kinase 2 regulates mitochondrial bioenergetics and impairs myostatin-mediated autophagy in muscle cells. *Am J Physiol Cell Physiol* 317: C674–C686
- Martinez-Lopez N, Garcia-Macia M, Sahu S, Athonvarangkul D, Liebling E, Merlo P, Cecconi F, Schwartz GJ, Singh R (2016) Autophagy in the CNS and periphery coordinate lipophagy and lipolysis in the brown adipose tissue and liver. *Cell Metab* 23: 113–127
- McWilliams TG, Prescott AR, Allen GFG, Tamjar J, Munson MJ, Thomson C, Muqit MMK, Ganley IG (2016) mito-QC illuminates mitophagy and mitochondrial architecture *in vivo*. *J Cell Biol* 214: 333–345
- McWilliams TG, Muqit MMK (2017) PINK1 and Parkin: emerging themes in mitochondrial homeostasis. *Curr Opin Cell Biol* 45: 83–91
- McWilliams TG, Prescott AR, Montava-Garriga L, Ball G, Singh F, Barini E, Muqit MMK, Brooks SP, Ganley IG (2018) Basal mitophagy occurs independently of PINK1 in mouse tissues of high metabolic demand. *Cell Metab* 27: 439–449
- Memme JM, Erlich AT, Phukan G, Hood DA (2019) Exercise and mitochondrial health. *J Physiol* <https://doi.org/10.1113/jp278853>
- Miller KN, Clark JP, Anderson RM (2019) Mitochondrial regulator PGC-1 α -modulating the modulator. *Curr Opin Endocr Metab Res* 5: 37–44
- Miwa S, Lawless C, von Zglinicki T (2008) Mitochondrial turnover in liver is fast *in vivo* and is accelerated by dietary restriction: application of a simple dynamic model. *Aging Cell* 7: 920–923
- Morita M, Gravel SP, Chenard V, Sikstrom K, Zheng L, Alain T, Gandin V, Avizonis D, Arguello M, Zakaria C et al (2013) mTORC1 controls mitochondrial activity and biogenesis through 4E-BP-dependent translational regulation. *Cell Metab* 18: 698–711
- Mottillo EP, Desjardins EM, Crane JD, Smith BK, Green AE, Ducommun S, Henriksen TI, Rebalka IA, Razi A, Sakamoto K et al (2016) Lack of adipocyte AMPK exacerbates insulin resistance and hepatic steatosis through brown and beige adipose tissue function. *Cell Metab* 24: 118–129
- Murakawa T, Yamaguchi O, Hashimoto A, Hikoso S, Takeda T, Oka T, Yasui H, Ueda H, Akazawa Y, Nakayama H et al (2015) Bcl-2-like protein 13 is a mammalian Atg32 homologue that mediates mitophagy and mitochondrial fragmentation. *Nat Commun* 6: 7527
- Nedergaard J, Golozoubova V, Matthias A, Asadi A, Jacobsson A, Cannon B (2001) UCP1: the only protein able to mediate adaptive non-shivering thermogenesis and metabolic inefficiency. *Biochim Biophys Acta* 1504: 82–106
- Novak I, Kirkin V, McEwan DG, Zhang J, Wild P, Rozenknop A, Rogov V, Lohr F, Popovic D, Occhipinti A et al (2010) Nix is a selective autophagy receptor for mitochondrial clearance. *EMBO Rep* 11: 45–51
- Okamoto K (2014) Organellophagy: eliminating cellular building blocks via selective autophagy. *J Cell Biol* 205: 435–445
- Palikaras K, Tavernarakis N (2014) Mitochondrial homeostasis: the interplay between mitophagy and mitochondrial biogenesis. *Exp Gerontol* 56: 182–188
- Palikaras K, Lionaki E, Tavernarakis N (2015a) Balancing mitochondrial biogenesis and mitophagy to maintain energy metabolism homeostasis. *Cell Death Differ* 22: 1399–1401
- Palikaras K, Lionaki E, Tavernarakis N (2015b) Coordination of mitophagy and mitochondrial biogenesis during ageing in *C. elegans*. *Nature* 521: 525–528
- Palikaras K, Daskalaki I, Markaki M, Tavernarakis N (2017) Mitophagy and age-related pathologies: development of new therapeutics by targeting mitochondrial turnover. *Pharmacol Ther* 178: 157–174
- Park JH, Kang HJ, Lee YK, Kang H, Kim J, Chung JH, Chang JS, McPherron AC, Lee SB (2015) Inactivation of EWS reduces PGC-1 α protein stability and mitochondrial homeostasis. *Proc Natl Acad Sci USA* 112: 6074–6079
- Pickles S, Vigie P, Youle RJ (2018) Mitophagy and quality control mechanisms in mitochondrial maintenance. *Curr Biol* 28: R170–R185
- Pirooznia SK, Yuan C, Khan MR, Karuppagounder SS, Wang L, Xiong Y, Kang SU, Lee Y, Dawson VL, Dawson TM (2020) PARIS induced defects in mitochondrial biogenesis drive dopamine neuron loss under conditions of parkin or PINK1 deficiency. *Mol Neurodegener* 15: 17
- Ploumi C, Daskalaki I, Tavernarakis N (2017) Mitochondrial biogenesis and clearance: a balancing act. *FEBS J* 284: 183–195
- Preston CC, Oberlin AS, Holmuhamedov EL, Gupta A, Sagar S, Syed RH, Siddiqui SA, Raghavakaimal S, Terzic A, Jahangir A (2008) Aging-induced alterations in gene transcripts and functional activity of mitochondrial oxidative phosphorylation complexes in the heart. *Mech Ageing Dev* 129: 304–312
- Puigserver P, Wu ZD, Park CW, Graves R, Wright M, Spiegelman BM (1998) A cold-inducible coactivator of nuclear receptors linked to adaptive thermogenesis. *Cell* 92: 829–839
- Puigserver P (2005) Tissue-specific regulation of metabolic pathways through the transcriptional coactivator PGC1- α . *Int J Obes (Lond)* 29(Suppl 1): S5–S9
- Rasbach KA, Schnellmann RG (2007) Signaling of mitochondrial biogenesis following oxidant injury. *J Biol Chem* 282: 2355–2362
- Rikka S, Quinsay MN, Thomas RL, Kubli DA, Zhang X, Murphy AN, Gustafsson AB (2011) Bnip3 impairs mitochondrial bioenergetics and stimulates mitochondrial turnover. *Cell Death Differ* 18: 721–731
- Ruas JL, White JP, Rao RR, Kleiner S, Brannan KT, Harrison BC, Greene NP, Wu J, Estall JL, Irving BA et al (2012) A PGC-1 α isoform induced by resistance training regulates skeletal muscle hypertrophy. *Cell* 151: 1319–1331
- Sandoval H, Thiagarajan P, Dasgupta SK, Schumacher A, Prchal JT, Chen M, Wang J (2008) Essential role for Nix in autophagic maturation of erythroid cells. *Nature* 454: 232–U266
- Scarffe LA, Stevens DA, Dawson VL, Dawson TM (2014) Parkin and PINK1: much more than mitophagy. *Trends Neurosci* 37: 315–324
- Scarpulla RC (1997) Nuclear control of respiratory chain expression in mammalian cells. *J Bioenerg Biomembr* 29: 109–119
- Scarpulla RC (2002) Nuclear activators and coactivators in mammalian mitochondrial biogenesis. *Biochim Biophys Acta* 1576: 1–14

- Scarpulla RC (2008) Nuclear control of respiratory chain expression by nuclear respiratory factors and PGC-1-related coactivator. *Ann N Y Acad Sci* 1147: 321–334
- Scarpulla RC, Vega RB, Kelly DP (2012) Transcriptional integration of mitochondrial biogenesis. *Trends Endocrin Met* 23: 459–466
- Schofield JH, Schafer ZT (2020) Mitochondrial ROS and mitophagy: a complex and nuanced relationship. *Antioxid Redox Signal* <https://doi.org/10.1089/ars.2020.8058>
- Shin JH, Ko HS, Kang H, Lee Y, Lee YI, Pletinkova O, Troconso JC, Dawson VL, Dawson TM (2011) PARIS (ZNF746) repression of PGC-1alpha contributes to neurodegeneration in Parkinson's disease. *Cell* 144: 689–702
- Stephan JS, Yeh YY, Ramachandran V, Deminoff SJ, Herman PK (2009) The Tor and PKA signaling pathways independently target the Atg1/Atg13 protein kinase complex to control autophagy. *Proc Natl Acad Sci USA* 106: 17049–17054
- Sterky FH, Lee S, Wibom R, Olson L, Larsson NG (2011) Impaired mitochondrial transport and Parkin-independent degeneration of respiratory chain-deficient dopamine neurons *in vivo*. *Proc Natl Acad Sci USA* 108: 12937–12942
- Sugiura A, McLelland GL, Fon EA, McBride HM (2014) A new pathway for mitochondrial quality control: mitochondrial-derived vesicles. *EMBO J* 33: 2142–2156
- Sun N, Yun J, Liu J, Malide D, Liu C, Rovira II, Holmstrom KM, Fergusson MM, Yoo YH, Combs CA *et al* (2015) Measuring *In Vivo* Mitophagy. *Mol Cell* 60: 685–696
- Uldry M, Yang W, St-Pierre J, Lin J, Seale P, Spiegelman BM (2006) Complementary action of the PGC-1 coactivators in mitochondrial biogenesis and brown fat differentiation. *Cell Metab* 3: 333–341
- Vafai SB, Mootha VK (2012) Mitochondrial disorders as windows into an ancient organelle. *Nature* 491: 374–383
- Valero T (2014) Mitochondrial biogenesis: pharmacological approaches. *Curr Pharm Des* 20: 5507–5509
- Vernia S, Cavanagh-Kyros J, Garcia-Haro L, Sabio G, Barrett T, Jung DY, Kim JK, Xu J, Shulha HP, Garber M *et al* (2014) The PPARalpha-FGF21 hormone axis contributes to metabolic regulation by the hepatic JNK signaling pathway. *Cell Metab* 20: 512–525
- Watanabe M, Yamamoto T, Kakuwata R, Okada N, Kajimoto K, Yamazaki N, Kataoka M, Baba Y, Tamaki T, Shinohara Y (2008) Synchronized changes in transcript levels of genes activating cold exposure-induced thermogenesis in brown adipose tissue of experimental animals. *Biochim Biophys Acta* 1777: 104–112
- Wei H, Liu L, Chen Q (2015) Selective removal of mitochondria via mitophagy: distinct pathways for different mitochondrial stresses. *Biochim Biophys Acta* 1853: 2784–2790
- Wei Y, Chiang WC, Sumpter Jr R, Mishra P, Levine B (2017) Prohibitin 2 is an inner mitochondrial membrane mitophagy receptor. *Cell* 168: 224–238
- Whitworth AJ, Pallanck LJ (2017) PINK1/Parkin mitophagy and neurodegeneration-what do we really know *in vivo*? *Curr Opin Genet Dev* 44: 47–53
- Wu Z, Puigserver P, Andersson U, Zhang C, Adelmant G, Mootha V, Troy A, Cinti S, Lowell B, Scarpulla RC *et al* (1999) Mechanisms controlling mitochondrial biogenesis and respiration through the thermogenic coactivator PGC-1. *Cell* 98: 115–124
- Wu H, Wang Y, Li W, Chen H, Du L, Liu D, Wang X, Xu T, Liu L, Chen Q (2019) Deficiency of mitophagy receptor FUNDC1 impairs mitochondrial quality and aggravates dietary-induced obesity and metabolic syndrome. *Autophagy* 15: 1882–1898
- Zhang CS, Lin SC (2016) AMPK promotes autophagy by facilitating mitochondrial fission. *Cell Metab* 23: 399–401